Earth-Science Reviews 138 (2014) 137–155

Contents lists available at ScienceDirect

Earth-Science Reviews

journal homepage: www.elsevier.com/locate/earscirev

# Construction of volcanic records from marine sediment cores: A review and case study (Montserrat, West Indies)

Michael Cassidy [a,*], Sebastian F.L. Watt [a,b], Martin R. Palmer [a], Jessica Trofimovs [c], William Symons [a], Suzanne E. Maclachlan [d], Adam J. Stinton [e,f]

[a] Ocean and Earth Science, University of Southampton, UK
[b] School of Geography, Earth and Environmental Sciences, University of Birmingham, Edgbaston, Birmingham B15 2TT, UK
[c] Queensland University of Technology, Brisbane, Australia
[d] British Ocean Sediment Core Research Facility, National Oceanography Centre, Southampton, UK
[e] Montserrat Volcano Observatory, Flemmings, W.I., Montserrat
[f] Seismic Research Centre, The University of the West Indies, St. Augustine, W.I., Trinidad and Tobago

ARTICLE INFO

*Article history:*
Received 17 May 2013
Accepted 12 August 2014
Available online 23 August 2014

*Keywords:*
Tephrostratigraphy
Tephrochronology
Eruption history
Cryptotephras
Tephra fallout
Reworked volcaniclastic

ABSTRACT

Detailed knowledge of the past history of an active volcano is crucial for the prediction of the timing, frequency and style of future eruptions, and for the identification of potentially at-risk areas. Subaerial volcanic stratigraphies are often incomplete, due to a lack of exposure, or burial and erosion from subsequent eruptions. However, many volcanic eruptions produce widely-dispersed explosive products that are frequently deposited as tephra layers in the sea. Cores of marine sediment therefore have the potential to provide more complete volcanic stratigraphies, at least for explosive eruptions. Nevertheless, problems such as bioturbation and dispersal by currents affect the preservation and subsequent detection of marine tephra deposits. Consequently, cryptotephras, in which tephra grains are not sufficiently concentrated to form layers that are visible to the naked eye, may be the only record of many explosive eruptions. Additionally, thin, reworked deposits of volcanic clasts transported by floods and landslides, or during pyroclastic density currents may be incorrectly interpreted as tephra fallout layers, leading to the construction of inaccurate records of volcanism. This work uses samples from the volcanic island of Montserrat as a case study to test different techniques for generating volcanic eruption records from marine sediment cores, with a particular relevance to cores sampled in relatively proximal settings (i.e. tens of kilometres from the volcanic source) where volcaniclastic material may form a pervasive component of the sedimentary sequence. Visible volcaniclastic deposits identified by sedimentological logging were used to test the effectiveness of potential alternative volcaniclastic-deposit detection techniques, including point counting of grain types (component analysis), glass or mineral chemistry, colour spectrophotometry, grain size measurements, XRF core scanning, magnetic susceptibility and X-radiography. This study demonstrates that a set of time-efficient, non-destructive and high-spatial-resolution analyses (e.g. XRF core-scanning and magnetic susceptibility) can be used effectively to detect potential cryptotephra horizons in marine sediment cores. Once these horizons have been sampled, microscope image analysis of volcaniclastic grains can be used successfully to discriminate between tephra fallout deposits and other volcaniclastic deposits, by using specific criteria related to clast morphology and sorting. Standard practice should be employed when analysing marine sediment cores to accurately identify both visible tephra and cryptotephra deposits, and to distinguish fallout deposits from other volcaniclastic deposits.



**Contents**



* Corresponding author at: National Oceanography Centre Southampton, University of Southampton Waterfront Campus, European Way, Southampton SO14 3ZH, UK. Tel.: +44 23 8059 6468.
*E-mail address:* m.cassidy@soton.ac.uk (M. Cassidy).

http://dx.doi.org/10.1016/j.earscirev.2014.08.008
0012-8252/

## 1. Introduction

The products of an individual subaerial volcanic eruption are often rapidly buried beneath later eruption products, eroded or covered by vegetation soon after their deposition, making it difficult to reconstruct comprehensive volcanic histories from terrestrial exposures alone. As a consequence, dispersed explosive-eruption products (tephra) sampled within marine- and lake-sediment cores are widely used to reconstruct explosive eruption records of volcanoes (e.g. Paterne et al., 1988; Ortega-Guerrero and Newton, 1998; Wulf et al., 2004, 2012; de Fontaine et al., 2007; Bertrand et al., 2008; Gudmundsdóttir et al., 2012). In making such reconstructions, it is important that explosive eruption deposits are correctly identified, and can be discriminated from volcaniclastic sediments deposited via other mechanisms (e.g. Ruddiman and Glover, 1972; Schneider et al., 2001; Trofimovs et al., 2006; Manville et al., 2009; Hunt et al., 2011). If this can be achieved, and if these tephra deposits are preserved within an environment of continuous sediment accumulation, then subaqueous sediment cores can be used to produce explosive eruption records that are more complete, and which have better age-constraints, than those typically derived from subaerial deposits. Marine and lacustrine sediments can thus provide a medium by which to assess the periodicity of eruptions and potential hazards posed by volcanoes, across a range of temporal and spatial scales (McGuire et al., 1997; Pyle et al., 2006; Kutterolf et al., 2008, 2013; Carel et al., 2011; Watt et al., 2013; Van Daele et al., 2014).

The interpretation of sediments containing volcaniclastic material is not without pitfalls (Boygle, 1999; Schneider et al., 2001; Juvigné et al., 2008; Gudmundsdóttir et al., 2011; Schindlbeck et al., 2013). In order to avoid erroneous or inconsistent identification of explosive volcanic eruption deposits, it is important that well-defined techniques are adopted for the analysis of volcaniclastic deposits within sediment cores. Inadequate detection techniques may overlook thin or dispersed tephra layers, that are invisible to the naked eye (cryptotephras), or misinterpret volcaniclastic sediments deposited via other mechanisms (Manville et al., 2009) as tephra fallout layers.

### 1.1. Rationale and aims

There have been considerable advances in the methods used to detect, date and characterise volcaniclastic deposits in the last few decades (Froggatt, 1992; Turney et al., 2004; Blockley et al., 2005; Gehrels et al., 2008; Manville et al., 2009; Lowe, 2011). However, subjective elements in the criteria used to identify a tephra layer deposited from an explosive volcanic eruption still remain.

Tephra deposits have been generally used for two broad applications, which differ in their spatial scales, and specifically in the typical distance of tephra sampling from the volcanic source. The first application involves the correlation of widespread (distal) deposits from very large (Plinian) and relatively infrequent explosive eruptions (e.g. Machida and Arai, 1983; Pyle et al., 2006). Volcanic ash may be transported vast distances. For example, glass shards from the El Chichón (Mexico) eruption in 1982 were identified in Greenland ice, ~10,000 km from the source (Zielinski et al., 1997). Such widespread deposits thus provide useful isochronous markers over thousands of square kilometres and are widely used in palaeo-climate studies (e.g. Allen et al., 1999; Lowe et al., 2008). Correlation of these distal deposits is aided by their deposition far from active volcanic sources, where volcaniclastic grains are a rare grain-type and where deposition via airfall may be the only plausible origin of volcaniclastic material (e.g. Matthews et al., 2012). It is thus possible to separate these grains from their host sediment (Blockley et al., 2005; Bourne et al., 2010) and to correlate them across widely-spaced sites using their glass or mineral chemistry (e.g. Kotaki et al., 2011; Matsu'ura et al., 2011; Smith et al., 2011; Albert et al., 2012). As well as providing chronological markers, such correlations provide constraints on the magnitude and frequency of large explosive eruptions.

The second broad purpose of tephra studies is to provide an explosive eruption record at individual volcanoes (or groups of volcanoes) (e.g. de Fontaine et al., 2007; Bertrand et al., 2008). These tephrostratigraphic studies are presented with a range of interpretational challenges, which are much less of an issue than for studies examining distal tephra deposits. Although cores sampled hundreds of kilometres from a volcano may still record multiple eruptions from a single volcano (Gehrels et al., 2006; Lane et al., 2012), construction of more comprehensive eruption records requires cores that are sampled relatively close (proximal; i.e. tens of kilometres) to the volcanic source (Bertrand et al., 2008; Carel et al., 2011; Van Daele et al., 2014). This is because the majority of explosive eruptions are too small to produce widespread tephra deposits. In proximal subaqueous environments, volcaniclastic-grains may be a common sediment type. Such environments are often sedimentologically and tectonically active, and discrete volcaniclastic deposits may be produced through a host of processes other than tephra fallout, including mass-flow or turbidite deposits derived from pyroclastic density currents, subaerial or submarine volcanic landslides, floods or lahars, or the reworking of submarine slope sediment (Boygle, 1999; Schneider et al., 2001; Gudmundsdóttir et al., 2011; Hunt et al., 2011; Schindlbeck et al., 2013). Additionally, multiple discrete deposits may have similar chemical compositions, because they are derived from the same magmatic system, meaning that glass or mineral analyses are less useful for inter-core correlations (Juvigné et al., 2008; although note that such problems may also be relevant, but under-appreciated, for the correlation of widespread distal deposits, cf. Lane et al., 2012). Deposits from small explosive eruptions may also produce tephra with a crystal-rich matrix, unlike the silicic glass of many Plinian events, which further hinders correlation via glass chemistry.

The challenges for the identification and analysis of tephra deposits in proximal cores, outlined above, can be divided into three areas:

1. Because of high-levels of background volcaniclastic sedimentation, dispersed throughout the cores, tephra fallout deposits that do not form discrete visible layers (i.e. cryptotephras) are difficult to identify or to distinguish from dispersed volcaniclastic material deposited by other mechanisms.
2. A wide range of processes can deposit volcaniclastic sediment, forming both discrete, visible horizons and dispersed accumulations. These include primary processes, which are derived directly from an explosive volcanic eruption, and can be divided into fallout deposits and pyroclastic-density-current derived deposits (e.g. Schneider et al., 2001; Trofimovs et al., 2006; Schindlbeck et al., 2013); and secondary deposits, which do not represent an explosive volcanic eruption (e.g. derived from a range of mass-movements), flows or floods (e.g., Boygle, 1999; Gudmundsdóttir et al., 2011). Distinguishing fallout deposits from other deposits may not be straightforward.
3. The chemical composition of tephra deposits is not necessarily useful for correlating between cores, due to multiple events of similar compositions and a possible absence of analysable glass (e.g. Juvigné et al., 2008; Kotaki et al., 2011). Correlation may thus require a combination of approaches.

In spite of these challenges, it may be possible to use a range of deposit characteristics (e.g. grain abundance, grain type, chemical composition, morphology) to differentiate between tephra fall deposits, primary deposits derived from pyroclastic density currents, and volcaniclastic deposits derived from other processes. Such a distinction is an essential first-step for the compilation of accurate and comprehensive explosive eruption records, and must be completed before more detailed correlation is attempted using chemical and stratigraphic characteristics. However, there are currently no clearly defined guidelines or approaches for making this distinction for cores sampled within volcanically-active regions (cf. Le Friant et al., 2008). Without a well-designed approach to address the challenges involved in interpreting subaqueous volcaniclastic deposits in such environments, there is a danger that erroneous eruption records may be produced.

Here, we test the effectiveness of widely-used techniques employed to identify tephra layers in marine sediment cores in regions close to the volcanic source (i.e. potentially subject to a range of styles of volcaniclastic deposition; Manville et al., 2009). In particular, we critically evaluate the capacity of these techniques to detect visible and invisible volcaniclastic layers, and to distinguish tephra fallout layers from volcaniclastic material deposited via other processes (e.g., derived from pyroclastic density current, lahars, landslides, fluvial action etc.). Our aim is to develop an objective approach that may be used to identify tephra fallout deposits in sediment sequences rich in volcaniclastic material, and thus aid in the production of more complete and accurate volcanic eruption records from sediment core samples.

We assess tephra-interpretation techniques through a detailed case study of a marine sediment core sampled ~55 km offshore Montserrat in the Lesser Antilles (Fig. 1). Montserrat is an ideal region for this type of study, because the surrounding seafloor has been extensively surveyed (Le Friant et al., 2004, 2009; Lebas et al., 2011; Watt et al., 2012a, b) and cored (Trofimovs et al., 2006, 2008, 2010, 2013; Le Friant et al., 2008, 2009, 2010; Cassidy et al., 2013, 2014), and the subaerial record of volcanism and igneous geochemistry is particularly well-constrained (Rea, 1974; Roobol and Smith, 1998; Harford et al., 2002; Zellmer et al., 2003; Smith et al., 2007; Cassidy et al., 2012). This earlier work has shown that marine volcaniclastic sedimentation around Montserrat encompasses a rich array of processes, and that the identification of tephra fall deposits within the stratigraphy is not a trivial task. By using a range of methods, and by drawing on existing data of Montserrat's deposits, we aim to produce an approach that can successfully identify tephra fall deposits within such environments. Our focus in this paper is principally on analytical techniques and their interpretation. We do not aim to improve the eruption record of Montserrat in this particular study, but use this single core to refine the techniques that are a pre-requisite to developing such eruption records in the future.

The structure of this paper is as follows: First, we outline the relevant terminology and discuss volcaniclastic sedimentation in marine settings. We then describe a range of methods that have been applied to our marine sediment core. We reiterate that our aim is to gauge the success of these methods in distinguishing tephra fallout deposits from other volcaniclastic deposits, which must be done before attempts at inter-core correlation are made. The success of each method is discussed in turn, and we then put forward an idealised approach for distinguishing tephra fallout deposits from other volcaniclastic deposits in sediment core samples. Our approach is particularly applicable in environments relatively proximal to volcanic sources, where cores are expected to be rich in volcaniclastic sediment that may have been deposited in a variety of ways.

### 1.2. Terminology

Tephrostratigraphic and tephrochronological studies require a multidisciplinary approach. Hence, we provide an overview of the terminology used herein, as variable use of nomenclature by researchers from different backgrounds can otherwise lead to ambiguities.

#### 1.2.1. Volcanology terms

"Tephra" is the collective term for the unconsolidated pyroclastic products formed by explosive volcanic processes. It includes all grain sizes from fine ash (<0.06 mm) to blocks and bombs (>64 mm) (Froggatt and Lowe, 1990; Lowe and Hunt, 2001). "Pyroclastic" is the collective term for clastic or fragmentary material, welded or non-welded that is explosively ejected from a volcanic vent (Froggatt and Lowe, 1990). "Cryptotephra" are tephra deposits that are not visible to the naked eye. They are often present as concentrations of glass shards or crystal fragments mixed with non-volcanic clasts (Lowe and Hunt, 2001; Turney et al., 2004). "Volcaniclastic" describes particles formed

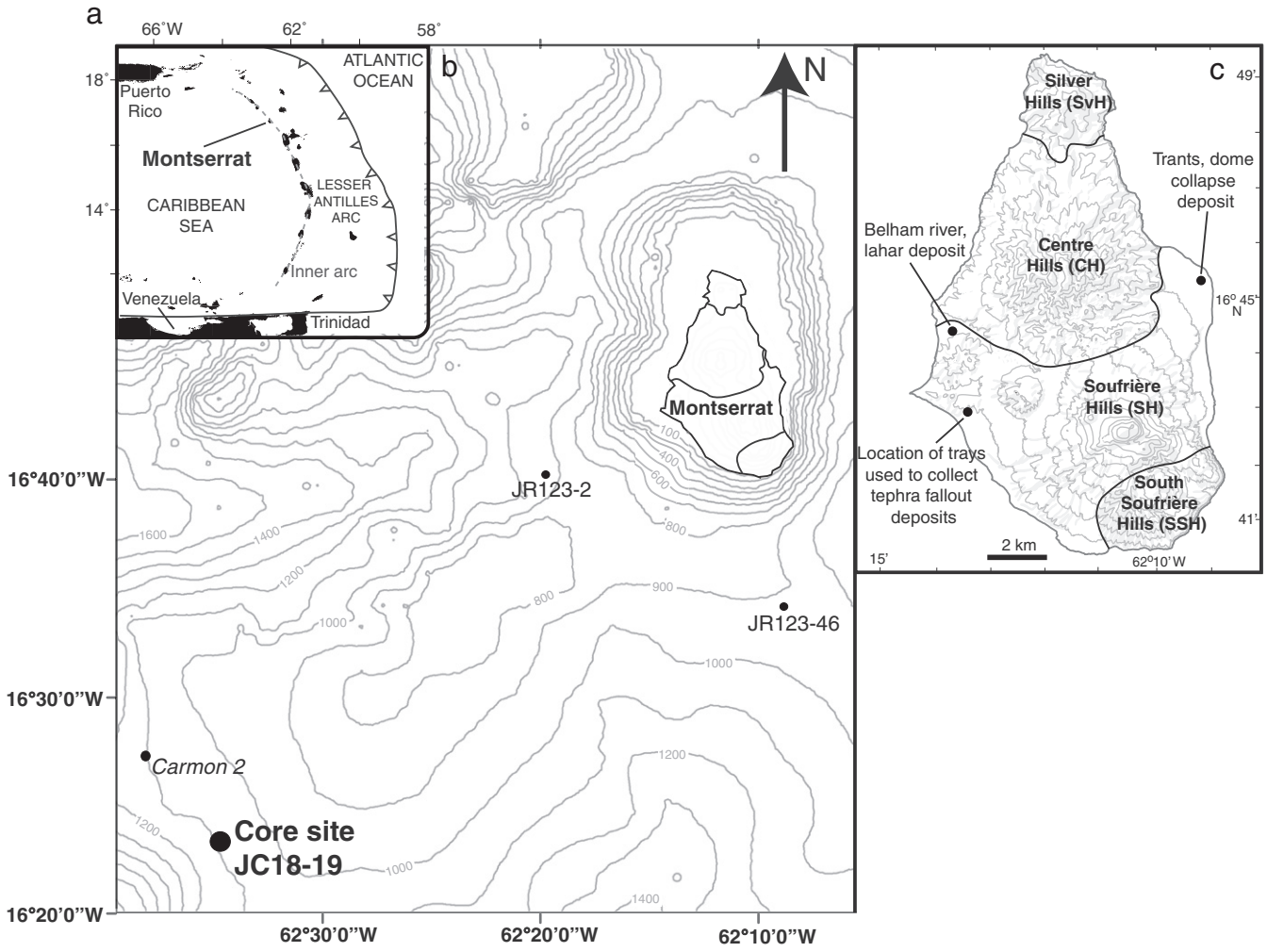


**Fig. 1.** (a) Location of Montserrat in the Lesser Antilles. (b) Site of the core at the focus of this study (JC18-19), is ~55 km offshore Montserrat. Known reworked volcaniclastic deposits were sampled from core JCR123-2 and JR123-46 for comparison. Carmon 2 is the core examined in the study by Le Friant et al. (2008) and plotted here for reference. (c) A detailed map of Montserrat showing the four different volcanic centres, including the locations of lahar, dome collapse and tephra fallout samples from the recent eruptions used in this study.

by the fragmentation of rocks or magma, that were originally derived from a volcanic eruption (Carey, 2000). Such particles may be reworked or primary, and could thus form by fragmentation of pre-existing deposits (e.g. via mass-wasting processes) as well as eruptive fragmentation. "Primary tephra deposits" preserve material formed by, and deposited contemporaneously with, a pyroclast-generating (explosive) volcanic eruption. They may be divided into tephra fallout and pyroclastic-density-current derived deposits. In contrast, "reworked volcaniclastic/tephra" deposits contain volcaniclastic material that has been eroded or remobilised after its initial deposition, and then transported and redeposited (Cas and Wright, 1987; Manville et al., 2009). "Tephra fallout" is the rain-out of clasts through the atmosphere from a plume generated during an explosive eruption (Walker et al., 1971; Houghton et al., 2000). Tephra can also be dispersed by pyroclastic density currents.

*1.2.2. Sedimentology terms*

"Turbidity current" refers to a dilute gravity flow of material, where fluid turbulence is the dominant support mechanism (Kneller and Buckee, 2000; Mulder and Alexander, 2001). Deposits from turbidity currents are termed turbidites and result from progressive aggradation, where clasts accumulate in a layer-by-layer fashion (Kuenen, 1966; Walker, 1969; Allen, 1971). This process commonly leads to vertical grading unless the flow becomes unsteady (Amy and Talling, 2006; Talling et al., 2007). Subaerial pyroclastic density currents can (partially) transform into turbidity currents upon entrance into the ocean (Trofimovs et al., 2006, 2008; Cassidy et al., 2013), although turbidity currents may also deposit volcaniclastic sediment via a range of other, non-eruptive processes (Schindlbeck et al., 2013).

*1.3. Volcanic sedimentation in oceanic settings*

Volcanic material can enter the ocean by: 1) tephra fallout from explosive volcanic eruptions; 2) primary volcanic flows, such as pyroclastic density currents; and 3) reworked volcanic material transported by subaerial and submarine gravity-driven mass movements (e.g. turbidity currents), gradual erosion by rivers, wind, ocean currents and, in colder settings, ice-rafted debris (IRD).

*1.3.1. Primary volcaniclastic deposits*

*1.3.1.1. Tephra fallout deposits.* Explosive eruptions can transport tephra large distances (Walker et al., 1971; Wilson and Walker, 1987), with the degree of magma fragmentation (grain-size distribution), weather conditions, and height of particle injection into the atmosphere all acting to control the distribution and extent of tephra fallout (Sparks et al., 1997). For these reasons, it is preferable to take multiple cores at varying proximities and directions from source to increase the likelihood of finding tephra deposits from that source, and to reduce the risk of an individual tephra layer being missed in reconstructions. Tephra fallout deposits are

the basis of tephrochronology, because they can be emplaced over a wide area and form a stratigraphic marker of equivalent time across all the sequences in which they are preserved (e.g. Pyle et al., 2006; Lane et al., 2012).

Tephra deposited in the ocean typically sinks at ~1–3 orders of magnitude faster than Stokes-Law settling due to the generation of vertical density currents (Carey, 1997; Manville and Wilson, 2004; Kandlbauer et al., 2013). This process leads to tephra deposits commonly exhibiting sharp bases in sediment cores, with bioturbated or gradational upper contacts. The rapid sedimentation of tephra deposits in seawater also reduces lateral ash transport in the water-column by ocean currents (Carey, 1997; Kandlbauer et al., 2013). Erosion by vigorous bottom currents or later gravitational flows may commonly erode and redistribute tephra deposits in the marine environment. Such processes may be particularly relevant within active volcanic arc environments, where water depths are shallower than in ocean basins and where complex topography may develop. For example, tephra fallout deposits from the Campanian Ignimbrite, in the Mediterranean Sea, suggest that tephra thickness varies according to the surrounding bathymetry (Engwell et al., 2014), and because submarine flows are commonly channelized in depressions, fallout tephras are more likely to survive erosion when they are emplaced on bathymetric highs. In less dynamic environments tephra fallout deposits in marine sediments are commonly normally-graded as they reflect the different sinking velocities of the different eruptive particles through the water column until they reach the ocean floor (Manville and Wilson, 2004). Additionally, akin to subaerial deposits, structures within tephra fallout deposits reflect the duration of an explosive eruption. Transitions or jumps in grading patterns can reflect changes in both the eruption parameters and/or wind conditions (e.g. Watt et al., 2009).

*1.3.1.2. Pyroclastic density current deposits.* Where the volcanic source is close to the shoreline, pyroclastic density currents may enter the oceans (e.g. following a lava dome collapse or collapse of a vertical ash plume). Volcaniclastic deposits formed by this mechanism are generally thicker than tephra fallout deposits (and thus more likely to be preserved). However, they commonly have erosional bases that can remove the underlying substrate, leading to the generation of an incomplete stratigraphic record, and are also far less laterally extensive than fallout deposits. They can therefore be missed during widely-spaced coring strategies, and are less useful as chrono-stratigraphic markers. Our main focus in this paper is therefore on identifying methods for successfully discriminating tephra fallout deposits from all other volcaniclastic deposits, because such deposits are not erosional, are often widely distributed, and can form stacked sequences of readily datable material.

*1.3.1.3. Cryptotephras.* Distal fallout deposits, and those generated from smaller eruptions, are commonly thin, fine-grained, and diffuse, and may be invisible to the naked eye. Such deposits are termed cyrptotephras, and can be notoriously difficult to identify within marine sequences. When deposited in areas where volcaniclastic sedimentation is usually absent, grains within cryptotephra deposits can be separated from the host sediment (Blockley et al., 2005; Stanton et al., 2010), and correlated chemically with their equivalent, visible tephra deposits (e.g., Gehrels et al., 2006; Bourne et al., 2010; Albert et al., 2012).

Cryptotephras do not simply occur because of ultra-distal deposition, but may originate via post-depositional reworking of originally thicker deposits, or may simply be derived from smaller eruptions from a more proximal source. The preservation of a tephra layer of any thickness is heavily dependent on the background sedimentation rate, and also on conditions such as the nature of the background sediments, bottom currents, biological activity and bottom water oxygen concentrations (Wetzel, 2009; Hembury et al., 2012). In areas of high burial rate, deposits thicker than 0.5 cm may be widely preserved, but elsewhere even deposits several centimetres in thickness may become reworked and dispersed within the sedimentary sequence (Wetzel, 2009), forming diffuse cryptotephras. Bioturbation by benthic organisms or reworking by currents can result in patchy preservation (Hunt and Najman, 2003; Manville and Wilson, 2004) and the formation of tephra lenses or "pods." Cores may thus fail to sample an intact portion of the tephra deposit. Moderate bioturbation can be detected by a blotchy appearance of tephra in sediment cores, but reworking may be so extensive as to visually homogenise the tephra with the background sediments (Hunt and Najman, 2003; Manville and Wilson, 2004).

Traditional methods of component-analysis and systematic grain-size measurements are laborious, and may be flawed in environments close to sites of active volcanism. In such settings, volcaniclastic grains are dispersed throughout cores and potentially deposited via a range of processes. The presence of diffuse volcaniclastic grains cannot therefore be assumed to represent a tephra fallout deposit. For the same reasons, the methods of extracting cryptotephra grains from ultra-distal deposits (Blockley et al., 2005) do not apply, because the entire sediment sequence is enriched in volcaniclastic material. Identification of cryptotephras in these environments requires that diffuse accumulations that originated as fallout can be discriminated from diffuse volcaniclastic sediment deposited via other processes. Given that the formation of the cryptotephra may involve the mixing of a primary fallout deposit with host sediment that itself includes volcaniclastic material, the identification and separation of the original, fallout tephra grains may be challenging.

One consequence of failing to identify cryptotephras in sediment sequences is that any attempt to reconstruct the volcanic evolution of a target region will be incomplete, and is likely to under-sample relatively smaller explosive eruption deposit. Hence, if possible, it is important to develop rapid, non-destructive identification techniques that allow cryptotephras to be unambiguously identified even in sediment cores with high levels of background volcaniclastic sediment.

*1.3.2. Reworked volcaniclastic deposits*

Volcanic material can be emplaced on the sea floor without an eruption occurring (Manville et al., 2009). Previously erupted material is continually transported into the oceans from volcanic regions through wind, surface water and wave action that gradually erode volcanic edifices and islands (Sigurdsson et al., 1980; Carey and Sigurdsson, 1984; Fisher and Schmincke, 1994; Reid et al., 1996; Le Friant et al., 2004). Thus, the background hemipelagic sediment in an active island arc may be rich in volcaniclastic material (cf. Fig. 2). This presents particular challenges for the identification of cryptotephras, and negates the application of methods that rely on an absence of volcaniclastic material in the host sediment (e.g. Blockley et al., 2005).

Stochastic events, such as floods or landslides, can also rapidly transport previously erupted material to the oceans and produce discrete volcaniclastic deposits over large areas (Moore et al., 1994; Masson et al., 2006). As well as forming debris avalanche or debris flow deposits, such events can evolve into poorly-sorted, mud-rich debris flows, or turbidity currents via flow dilution (c.f. Mulder and Cochonat, 1996; Ilstad et al., 2004; Bryn et al., 2005), and may appear in marine sediments as thick (up to several metres; Rothwell, 1992), coarse-grained and far-reaching turbidites (>1000 km; Rothwell, 1992; Piper et al., 1999; Fine et al., 2005), with significant basal erosion (Garcia, 1996; Wynn and Masson, 2003; Masson et al., 2006; Hunt et al., 2011). Although widespread, the distribution of these deposits is ultimately subject to topographic controls, in contrast to tephra fallout deposits.

Lahars may distribute primary volcaniclastic material into seawater years after the original eruption, and may also entrain older volcanic material en route to the ocean. Like deposits derived from pyroclastic density currents, their related marine deposits are often thick in proximal locations relative to tephra fallout deposits, but are far less laterally extensive.

Volcaniclastic mass-flow deposits may be distinguished from tephra fallout deposits by the presence of tractional structures, such as cross-

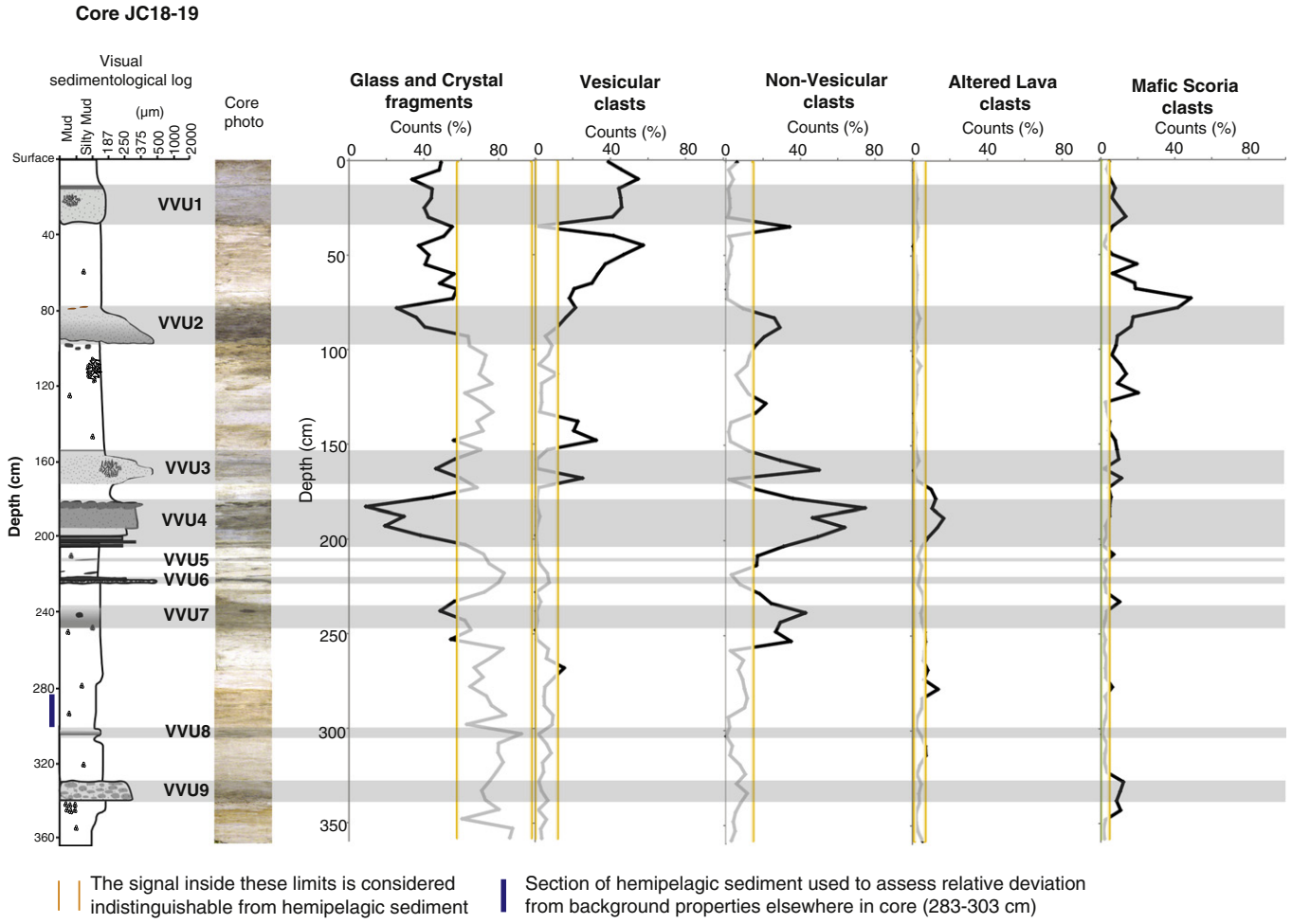


**Fig. 2.** Sedimentological log of the core (left), with visible volcaniclastic units highlighted and extrapolated in grey. This figure shows the component analysis throughout the core by point counting. Depth in cm is the depth below the seafloor.

and planar-laminae, and by graded-bedding, mud caps, erosive bases and/or poor-sorting (Bouma, 1962; Kneller and Buckee, 2000; Mulder and Alexander, 2001). However, the distal, thin, portion of flow deposits may not show such features, and may be much harder to distinguish from tephra fallout deposits. Additionally, it may be difficult to distinguish turbidites derived from pyroclastic density currents (i.e. primary flow deposits) from other mass flows transporting volcaniclastic sediment. Deposits from these events may also become dispersed via reworking, and form diffuse cryptotephra-like accumulations, which may be difficult to distinguish from true cryptotephras, derived from fallout.

The presence of ice-rafted debris (IRD) in marine sediments arises from the release of sediment frozen into the base of icebergs that is released as the ice drifts into warmer waters and melts (Heinrich, 1988; Bond et al., 1992). This sediment may include volcanogenic material (Ruddiman and Glover, 1972), but its accumulation through deposition of IRD can be distinguished from tephra fallout deposits by their poor-sorting, that may include large drop stones (Abbott et al., 2011).

Volcanic eruptions are geologically short-lived events, when compared to the periods between eruptions. During dormant intervals, a volcano is subject to erosion, transportation and redeposition of previously erupted material. For island arc volcanoes, ~90% of volcaniclastic material may be remobilised, compared to <40% for intra-plate oceanic islands such as Hawaii, and <10% from mid-ocean ridges (Carey, 2000). This behaviour accords with observations that volcanogenic material is widely disseminated in sediments surrounding island arc volcanoes (Reid et al., 1996). If the aim of a study is to reconstruct the eruption history of a volcano, it is important to distinguish tephra fallout deposits from all other volcaniclastic deposits, so as to avoid interpretations that contain spurious eruptive episodes.

### 1.4. Montserrat: the natural laboratory

Montserrat lies in the northern part of the Lesser Antilles island arc chain (Wadge, 1984; DeMets et al., 2000) (Fig. 1). The major components of deep water sediment in this region are volcaniclastic silt and clay, redeposited shallow-water carbonate detritus, pelagic carbonate, and windblown dust from Africa (Reid et al., 1996). Sigurdsson et al. (1980) estimate that 527 $km^3$ of volcanic material (285 $km^3$ D.R.E. — Dense Rock Equivalent) has been erupted from the Lesser Antilles island volcanoes in the last 100 ka. The majority of this material (84%) has been transported into adjacent marine basins and deposited as volcanogenic sediments, and is indicative of the impact of volcanism on marine sedimentation in island arcs.

Montserrat comprises four volcanic centres and has been active for at least 2.6 Ma. Most recently, this activity has originated from the currently active Soufrière Hills (282 ka to present), with an interlude of volcanism at South Soufrière Hills (SSH) (128–131 ka) (Harford et al., 2002). The subaerial record of volcanism at these two centres suggests eight active episodes, dating from 174 ka (Rea, 1974; Roobol and Smith, 1998; Harford et al., 2002; Smith et al., 2007; Cassidy et al., 2013). Studies of the history of Montserrat volcanism using submarine deposits have only been undertaken recently (Le Friant et al., 2008; Trofimovs et al., 2010, 2013; Cassidy et al., 2013, 2014). The most

ambitious of these studies has been a submarine tephrochronology record constructed for the Soufrière Hills volcano by Le Friant et al. (2008) using a distal marine sediment core, 55 km south west of Montserrat. In this study, eruptive episodes were detected by point counting the abundance of different types of volcanic clasts (glass shards, dense- and poorly-vesiculated juvenile clasts, crystals, vesicular juvenile clasts and lithics) at 10 cm intervals, except for volcaniclastic-rich zones, where the core was sampled every 5 cm. Micropaleontology–biostratigraphy and $\delta^{18}O$ isotope analyses of bulk carbonate samples measured throughout the core were used to date the volcanic horizons, which spanned the last 250 ka. The background hemipelagic sedimentation rate at this site is ~1–3 cm/kyr, and a 5-cm sampling frequency therefore yields ages with an uncertainty of $\sim\pm5$ kyr for identified volcaniclastic horizons. Intervals containing >16% glass-shard abundance were taken to indicate their derivation from an open-vent explosive eruption. Similarly, any interval containing >28% abundance of dense and poorly-vesiculated clasts was interpreted to be derived from a dome-forming eruption. Using this method, Le Friant et al. (2008) identified eight dome eruptions (five of which were correlated to dated subaerial domes or related pyroclastic flow sequences on Montserrat) and six open-vent explosive eruptions (which do not correspond with any documented eruptive deposits in the subaerial record). Sediment sequences with low abundances of volcanic material were interpreted to represent periods of dormancy or low activity, which typically extended for durations of ~10 kyr (Le Friant et al., 2008).

The current phase of activity on Montserrat provides a unique opportunity to study pyroclastic material entering the ocean. The subaerial expression of the eruption has been monitored in unprecedented detail, with timing, volume and flow dynamic data all recorded for individual pyroclastic flows (Barclay et al., 1998; Cole et al., 1998; Murphy et al., 1998, 2000; Sparks et al., 1998, 2000; Young et al., 1998; Calder et al., 1999; Melnik and Sparks, 1999; Voight et al., 1999; Couch et al., 2001, 2003; Zellmer et al., 2003; Herd et al., 2005). In addition, the combined study of subaerial flow conditions into the ocean with in-situ deposit morphology derived from marine sediment cores during the current eruption has provided valuable insights into submarine pyroclastic flow emplacement dynamics (Trofimovs et al., 2006, 2008, 2013; Le Friant et al., 2009, 2010). Thus, the excellent core coverage around Montserrat and the detailed subaerial eruption history provide a comprehensive background for the study presented here.

## 2. Methods

Core JC18-19 was collected on research cruise JC18 of the RRS James Cook (2007), using a gravity corer. The core was sampled ~55 km SW from Montserrat, in the prevailing wind direction and on a topographic high (water depth: 1130 m) (Fig. 1), in an attempt to exclusively target tephra fallout samples. The core location lies on relatively flat seafloor that gradually deepens from depths of ~700 m off the south flank of Montserrat. The core recovered 3.6 m of predominantly fine-grained (mud, silt and some sand) sediment in a 10-cm diameter core barrel. The core was housed in refrigerated storage at the British Ocean Sediment Core Facility (BOSCORF), based at the National Oceanography Centre (NOC), Southampton, UK prior to study. Sediment logging and photographs of JC18-19 allowed the initial identification of nine Visible Volcaniclastic Units (VVU1-9; Fig. 2).

### 2.1. Component analysis

Samples of ~0.5 $cm^3$ were taken at 3 cm intervals throughout core JC18-19 and dried at 60 °C. The samples were then washed with deionised water over a 63 μm sieve to remove the fine-grained hemipelagic component and 2.5 ml of acetic acid (20%) was added to the sample and left for 2 hours to dissolve the biogenic carbonate. The samples were then washed over a 63 μm sieve and dried in an oven at 55 °C. Aliquots of individual samples were placed on a gridded microscope slide. An average of 400 individual grains were point-counted and divided into five categories after the classification of Le Friant et al. (2008) (the bioclastic component was not included in this study). The five categories are as follows: (1) Volcanic glass shards and crystal fragments, which are fine-grained particles formed by the explosive disruption of magma; glass and crystals were combined as they are often difficult to distinguish without a polarising microscope when they are fine-grained and fragmental (Enache and Cumming, 2006); (2) vesicular clasts, which are unaltered pumiceous clasts formed by the exsolution of dissolved gases from magma; (3) non-vesicular lava clasts which, in this instance, are likely to originate from dome-forming eruptions; (4) altered lava clasts (i.e. with red or brown discolouration), which have been altered by hydrothermal fluids and gases; (5) mafic scoria clasts, which are vesicular and darker than the andesitic lava clasts. Examples of these subdivisions can be found in Fig. 5 of Cassidy et al. (2013).

### 2.2. Grain size

JC18-19 was sampled at 3 cm intervals for laser diffraction grain size analysis. Samples were added to 25 ml of RO water with a 0.05% sodium hexametaphosphate dispersant and left on a shaking table overnight. The dispersed sediment solutions were analysed using a Malvern Mastersizer 2000 particle size analyser, which is able to measure 0.02 to 2000 μm grain sizes. The particles are kept in suspension by in-built stirrers and the sample is pumped continuously through the Malvern analyser to ensure random orientation of the particles relative to the laser beam. Light obscuration was between 10 and 20%. Standard materials with mean diameters of 32 and 125 μm were used to monitor accuracy, while three repeat runs for each sample were used to monitor precision (reported at <0.5% SD).

### 2.3. Core scanning

#### 2.3.1. Magnetic susceptibility

Magnetic susceptibility is a commonly used, non-destructive tool for identifying tephra horizons in sediment cores (e.g., Hodgson et al., 1998; Takemura et al., 2000; Rasmussen et al., 2003; Kutterolf et al., 2008; Vogel et al., 2010). The GeoTek™ MSCL-XYZ multi-sensor core logger, based at BOSCORF, was used to measure magnetic susceptibility at 0.5 cm intervals on split cores using a Bartington MS2E point sensor (Rothwell and Rack, 2006). The interval distance was chosen to provide (slightly overlapping) high spatial resolution.

#### 2.3.2. Colour spectrophotometry

Colour spectrophotometry is a non-destructive method, capable of sampling at 3 mm resolution. A Konica Minolta colour spectrophotometer mounted in the GeoTek™ MSCL-XYZ logger measures reflectance from very near UV wave lengths through the visible light spectrum and into the very near IR range (wavelengths 360–740 nm) in 10-nm spectral bands, and was employed at 0.5 cm intervals. The resultant data record the optical properties of the sediment, where L* and greyscale represent lightness and reflectance gradients (0 for black to 100 for pure white), respectively. The actual colour (hue) is expressed as a* (negative values are red, positive is green) and b* (negative for blue and positive for yellow) (Nederbragt et al., 2006). This technique has been used in several studies to detect tephra layers in conjunction with other methods (Caseldine et al., 1999; Gehrels et al., 2008), but it has been noted that very low concentrations of shards and highly-dispersed tephra layers may not be resolvable from the background variability of non-volcanogenic sediments.

#### 2.3.3. XRF-core scanning

The bulk geochemical composition (semi-quantitative) of the sediment was determined by XRF core scanning (ITRAX™ COX Ltd.; Croudace et al., 2006) at BOSCORF. A spatial resolution of 1–3.5 mm

and a molybdenum X-ray tube was used, set at 30 kV and 30 mA and a dwell time of 40 s. The surface of split cores must be carefully flattened to reduce the effects of surface roughness and improve the signal-to-noise ratio of XRF logging records. Repeated scans of intervals of core JC18-19 within this study have shown that the ITRAX XRF core scanner produces reproducible results (generally <10% SD) at sub-mm to mm scales for the elements reported in this study (Kylander et al., 2012). The results are presented as log ratios to emphasise the relative changes in chemical compositions along the length of the sediment core (Weltje and Tjallingii, 2008). Ca and Sr were used as denominator elements as they yielded the highest intensities in sediments of JC18-19 (reflecting the dominance of hemipelagic carbonate in the background sediments) and showed the highest contrast between the (visible) volcanic units and the background sediment. Mn, Fe, Ti, K, and Si were used as proxies for volcaniclastic material, as these elements are found in the major minerals (feldspars, pyroxenes, amphiboles, titanite, magnetite) and groundmass that comprise the Montserrat volcanic rocks and have low concentrations in hemipelagic sediments.

Although no statistically significant correlation was observed between the mean grain size and XRF data, it is important to note that the ITRAX data are semi-quantitative and require calibration against matrix-matched standards (in the same manner as conventional XRF analyses) if accurate elemental data are required. The purpose of this study was not, however, to obtain accurate concentration data for individual layers, but rather to identify relative down-core changes in compositions that might reflect variable abundance of volcanic material. In this context, XRF core-scanning is useful as it is a rapid, non-destructive and high-resolution technique that has, for example, previously been used in palaeoclimate (Palike et al., 2001) and tephrostratigraphy studies (Brendryen et al., 2010; Vogel et al., 2010; Kylander et al., 2012).

#### 2.3.4. X-radiography

This technique provides a digital image of internal structure and physical property changes within a split core section, which are measured by the ITRAX instrument using optical and radiographic line cameras. The X-rays used to irradiate the core section are generated from a 3 kW Mo target and focused through a flat glass capillary waveguide to allow high-resolution measurement (down to 200 μm step size) (Croudace et al., 2006; Rothwell and Rack, 2006). The radiograph was generated at a setting of 60 kV and 50 mA with a dwell time of 800 ms. While this method has also been used in other studies (Lowe, 1988; Dugmore and Newton, 1992; Turner et al., 2008), its success in detecting tephra layers has been variable.

### 2.4. Image analysis

Image analysis of volcaniclastic grains from both visible deposits and potential cryptotephras was undertaken to determine whether these horizons represented primary tephra fallout deposits or other volcaniclastic deposits. Samples were wet-sieved at 63 μm and the carbonate dissolved using 20% acetic acid. The remaining material was cleaned with deionised water, dried and photographed under a stereo microscope with an integrated digital camera (Leica EZ4D). White paper was chosen as the background, as this provided the best contrast with volcanic clasts, except for pumice-rich samples, where a black background was used. The images were processed with ImageJ (Rasband WS, 1997–2012, http:imagej.nih.gov/ij) software. This included calibrating the scale, transforming the original image into an 8 bit, binary colour image and adjusting the threshold to accurately define the edges of the clasts. The "magic wand tool" was used to automatically trace around the clasts that retained their original shape/roughness during the image processing. The area, aspect ratio (longest axis/shortest axis) and perimeter were measured for 200–300 grains for each sample (~8–10 images), to provide statistically reproducible results. The grain size data was transferred into the Gradistat program (Blott and Pye, 2001) to determine sorting coefficients using the Folk and Ward (1957) method (geometric).

### 2.5. Glass geochemistry via electron microprobe

Major-element compositions of glass within vesicular volcanic clasts were determined using the Cameca SX100 electron microprobe at the University of Bristol, U.K. A range of silicate glass (e.g. basalt to rhyolite) standards was used for calibration of the spectrometers. Quantitative determinations of elements were made using the wavelength dispersive system with TAP, PET and LIF crystals. All analyses used an accelerating voltage of 15 kV, a 10 μm spot size, and a beam current of 4 nA, with counting times of 50–200 s per analysis. During glass measurements, Na peaks were counted first to avoid significant migration during the run. Accuracy was in general better than 3% for most elements, based on repeat analyses of EMPA basaltic secondary standard and by comparison with reference concentrations for the standard, with the exception of $TiO_2$, $K_2O$, and $P_2O_5$ which were better than 20–35%. Precision was typically <5% for all oxides.

## 3. Results and discussions of analytical methods

### 3.1. Methods testing

Sediment logging and digital photography revealed differences in the colour, grain type, grain size, nature of the upper and lower contacts, and visual appearance for several layers within JC18-19, leading to the identification of 9 visible volcaniclastic units — VVU1–VVU9 deposits (Figs. 2, 3 and 4). Note, however, that these are not necessarily primary tephra fallout deposits, as they may comprise volcaniclastic material derived from pyroclastic density currents or from secondary volcaniclastic mass-flow processes.

Each of the methods outlined above yields a numerical value (e.g. magnetic susceptibility, % components, etc.), which is related to the concentration of volcaniclastic material within the core. However, JC18-19 contains at least 7% volcaniclastic material disseminated throughout the background sediment. This estimate was derived by acidifying a sample to separate volcaniclastic from biogenic clasts, and calculating the difference in weight, and then "ground-truthed" by point counting. Hence, assigning a threshold to these values in order to distinguish between deposits from volcanic events and the continual dispersal of volcaniclastic sediment is not trivial. Indeed, this issue is likely common to all ocean sediments lying in areas influenced by deposition of volcanic material. Such areas may not simply be restricted to locations immediately around active island volcanoes, as exemplified by estimates that ~25% of Pacific Ocean sediment comprises volcanogenic material (Straub and Schmincke, 1998).

The key criterion for developing a method for identifying volcanic events from marine sediment core analyses is that it should be sufficiently objective to yield consistent results when applied to different areas by independent observers. As a means to achieving this objective, an approach is suggested based on first defining the inherent variability in the signature of local background sediment, generated by each analytical method.

The first step was to use visual inspection to identify sections of core that lacked obvious volcanogenic layers, and then to examine the analytical data obtained from these sections to identify a section of core that showed the least variation in these data. Using this approach, the 283–303 cm section of core was selected as the background type-section (highlighted as a blue line in Figs. 2, 3 and 4). Any signal lying outside the mean ± 2 standard deviations of the signal within this background section is then deemed to represent a departure in sediment properties from the background (the thresholds are shown as orange lines in Figs. 2–5). This represents a 95% (2σ) confidence level to distinguish a signal (i.e. non-hemipelagic material) from noise in the background sediment, and is an approach which is analogous to standard

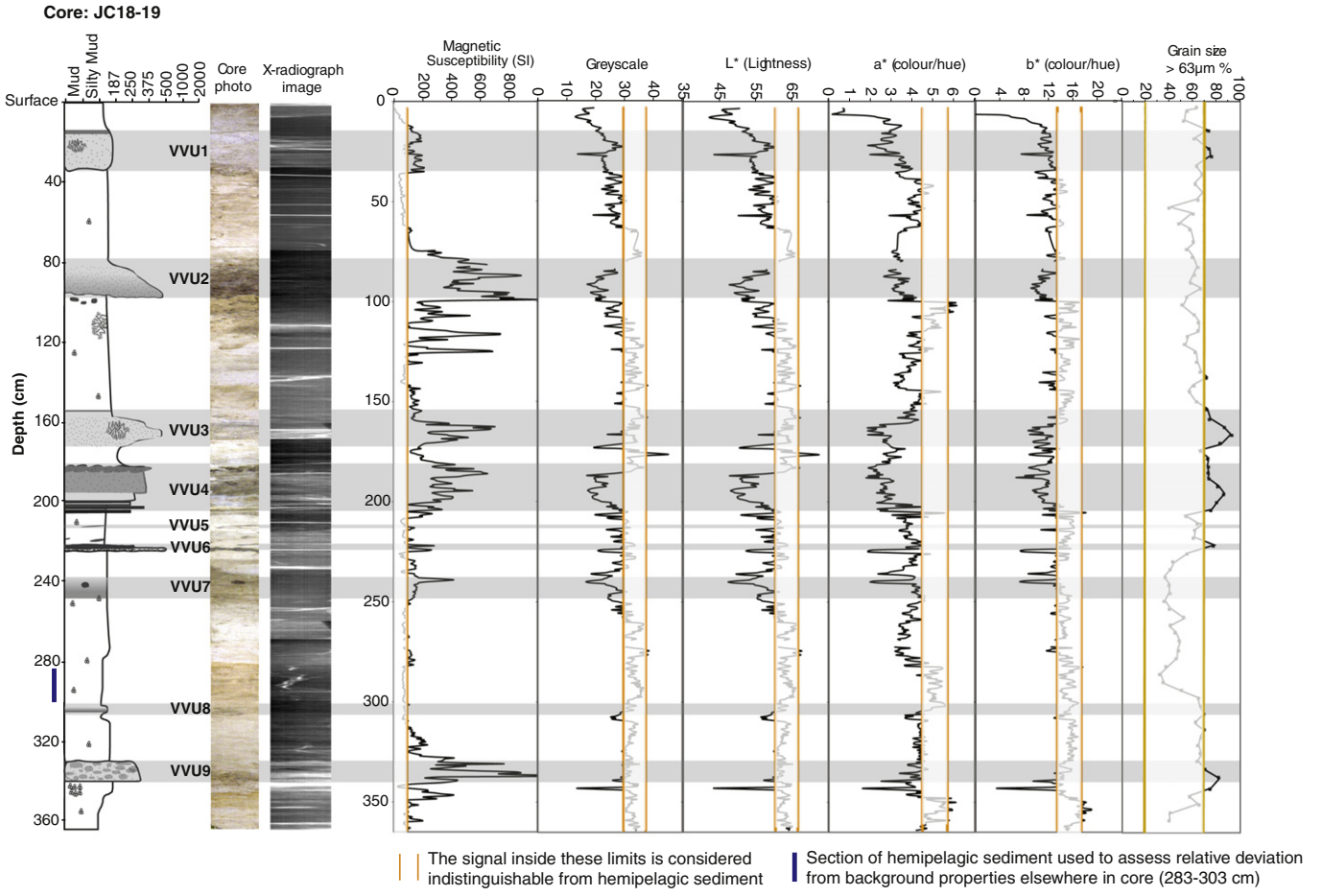


**Fig. 3.** Sedimentological log of the core (left), with visible volcaniclastic units highlighted and extrapolated in grey. X-radiograph images, magnetic susceptibility, colour spectrophotometry and grain size data are plotted for comparison. Depth in cm is the depth below the seafloor.

practice in analytical chemistry, whereby detection limits are defined from analyses of blank samples (Currie, 1968). It is important to note, however, that at this stage identification of anomalous sediment sections relative to this background section does not necessarily imply the presence of a tephra layer.

Positive or negative deviations from the signal thresholds are defined as "peaks." The fidelity with which these peaks relate to volcaniclastic horizons can then be assessed by comparison with the visually-identified VVU layers (Figs. 2–4; Table 1), as discussed below. Hence, we can judge the capacity of each technique to successfully identify volcaniclastic layers.

*3.1.1. Component analysis by point counting*

The volcanic clasts in the background sediment section are dominated by glass and crystal fragments (Fig. 2). Hence, high % counts of the other volcanic components yield peaks in the sedimentary record. This observation highlights one of the problems faced in identifying cryptotephra in regions where dispersed volcaniclastic grains form a component of the normal background sedimentation. Cryptotephras are typically identified by accumulations of glass shards (Blockley et al., 2005), but the presence of such grains in the background sediment means that component analysis is a relatively weak means of identifying cryptotephra layers in such environments.

Peaks in the % count of non-vesicular clasts (NVC) correspond most closely to the VVU layers (Fig. 2), with these peaks showing at least some overlap with 5 out of 9 of the VVU layers (Table 1). Thus, 61% of the total interval occupied by the VVU layers coincides with peak values in the NVC signal, and 71% of all the NVC signal peak values occur within the VVU bands (Table 1). The question as to whether the remaining 29% of the NVC peak values relate to cryptotephra layers will be considered below, but using clast componentry to resolve this is not straightforward. For example, because Plinian eruption deposits are generally dominated by glass and crystal fragments, which are also common in the background sediment, and because the carbonate proportion of the analysed sediments has been dissolved, Plinian deposits cannot readily be distinguished from the background signature by component analysis.

The use of component analysis is also problematic because the requirement for the total to add to 100% means that one or more volcanic clast type will always have a high abundance. The use of relative concentrations also means that an apparent increase in abundance of any one component does not necessarily reflect an increase in its accumulation rate. Instead, counts of a component per volume or weight sampled (e.g. glass shards per $cm^3$) should be used as standard when employing this technique (c.f. Wastegard and Davies, 2009). Finally, although component analysis may be a powerful method for identifying tephra horizons in regions where volcaniclastic material does not form part of the normal background sediment, it is still limited by its sampling resolution and it is very labour-intensive. Sufficient numbers of samples must be taken from a core to capture all the volcanic events (i.e., discrete deposits with thicknesses narrower than the sampling interval may be missed), and within any one sample enough grains must

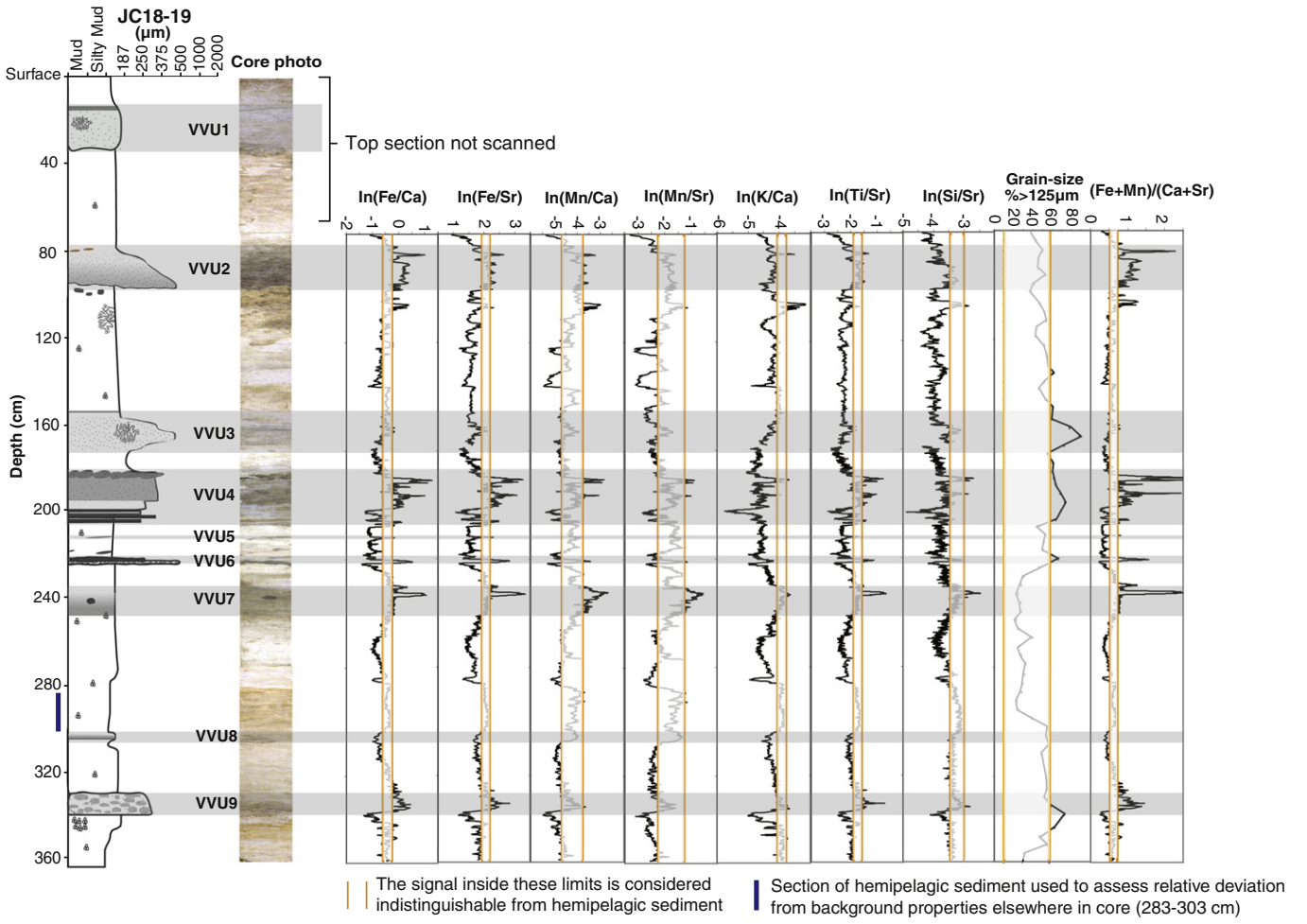


**Fig. 4.** Sedimentological log of the core (left), with visible volcaniclastic units highlighted and extrapolated in grey. Different geochemical ratios are plotted from the XRF core scanning data (via the ITRAX instrument). Grain size is plotted for comparison with XRF core scanned data. Depth in cm is the depth below the seafloor.

be counted to yield statistically significant data. In practice, it is not feasible to point count an entire core or to continually sample at high resolution.

### 3.1.2. Grain size measurements

Grain size measurements are destructive and slow compared with core scanning techniques, such as magnetic susceptibility. As with component analysis, sampling resolution is a trade-off between the time taken to perform the analyses, the desirability of preserving core material and the need to detect thin tephra layers. Again, this approach is limited in settings where the background sediment contains terrigenous material of similar grain-size to tephra fallout deposits. For example, it is not clear that any tephra deposits within JC18-19 would be of consistently distinct grain-size from either the background sediment or non-primary volcanic deposits such as turbidites. The shape (e.g., skewness and kurtosis) of the grain-size distribution may vary (due to sorting of the deposit), but this can be disrupted by bioturbation, rendering the technique weak for cryptotephras, which are by definition mixed with the background sediment.

The background-sediment type section shows some variability in % grain-size >63 μm (Fig. 3), but there are no negative deviations from the threshold values, suggesting that the background sediment region is generally the finest-grained part of the core. Five of the VVU contain sufficiently coarse grains to form peaks in this signal, but others are of near-identical grain-size to the surrounding sediment. Hence, this technique is unlikely to successfully detect cryptotephras, except in regions where the background sediment is very fine-grained pelagic clays. Only a small proportion of the signal forms peaks (26%), suggesting that when a peak does occur it warrants further investigation, and can be confidently assumed to represent a departure from normal background sedimentation, with most (68%) of the grain-size peaks overlapping with the VVU bands (Table 1). Hence, this technique can provide information about the sedimentology of the core that is useful for detecting turbidite sequences, and grain-size measurements are an important quality control on the XRF core scanning (Fig. 4), as the signal from the latter can be affected by changes in grain size.

### 3.1.3. Magnetic susceptibility

Magnetic susceptibility measurements are fast and non-destructive, but their spatial resolution is generally limited to ~0.5 cm. In addition, cryptotephras are often diffusely dispersed within hemipelagic sediment, and may not be present in sufficient quantities to produce a strong magnetic signal. Cryptotephras are also commonly dominated by glass shards, and because magnetic susceptibility reflects the volume of magnetic minerals (Blum, 1997), this may also weaken their signal. Hence, only positive deviations from the threshold for magnetic susceptibility are considered significant.

Peaks in magnetic susceptibility (MS) overlap with eight out of the nine VVU layers, which is the best success rate of any of the methods (Table 1). Unlike other techniques, the MS peaks also tend to span the full thickness of each VVU layer (peaks occupy 92% of the VVU sections and in some cases fit closely to the layer boundaries; Fig. 3). Although

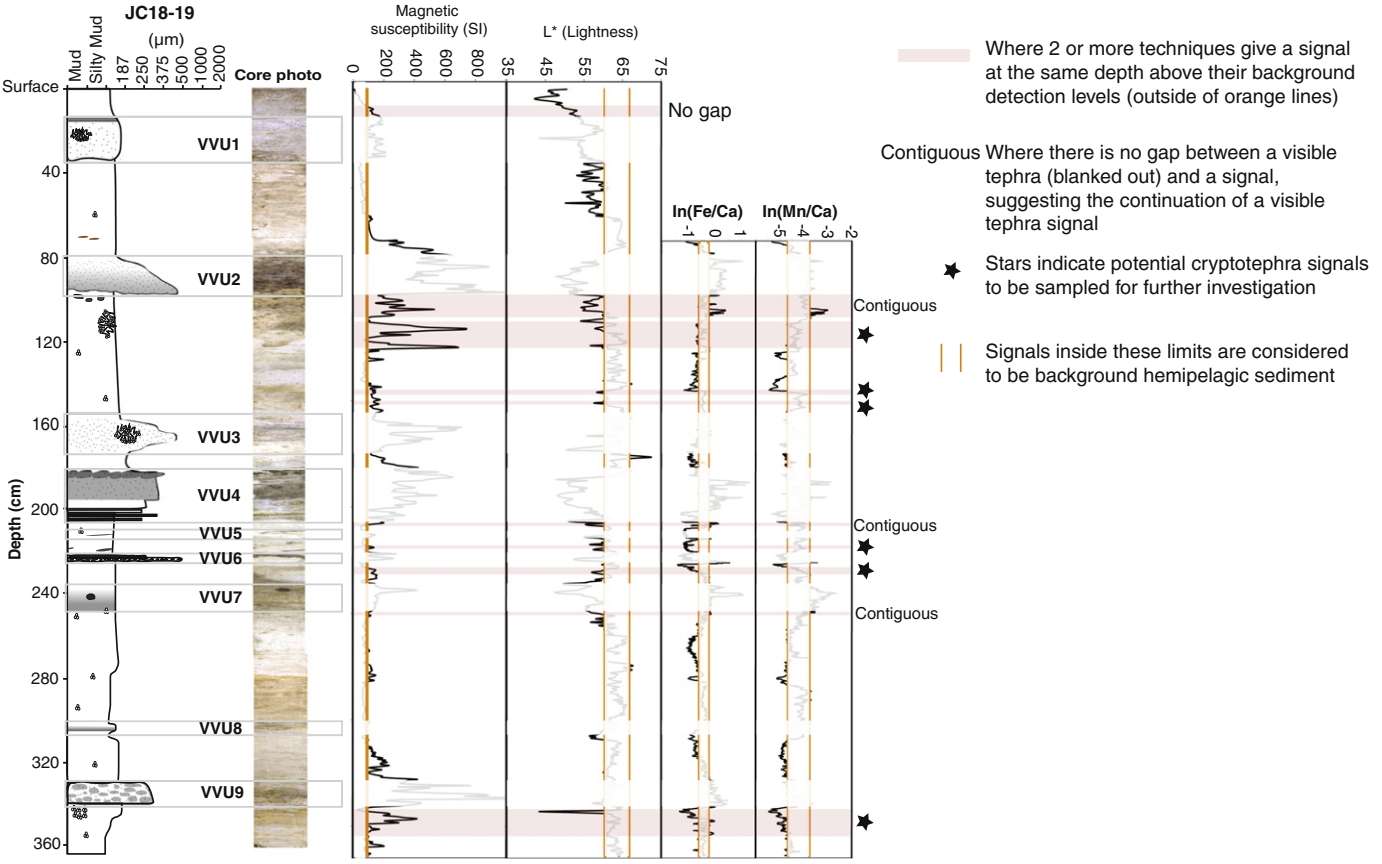


**Fig. 5.** Sedimentological log of the core (left). Magnetic susceptibility, L* (colour spectrophotometry) and XRF core scanned data (Ln(Fe/Ca) and Ln(Mn/Ca)) are plotted as these represented the most efficient techniques for detecting volcaniclastic material in the cores (Table 1). The visible volcanic units are faded out, so to highlight the peaks which fall outside these units in order to detect the non-visible volcaniclastic/cryptotephra units. Depth in cm is the depth below the seafloor.

MS appears to be a useful technique for identifying volcaniclastic horizons, it should be noted that 67% of the entire MS signal exceeds the threshold (i.e. forms peaks). Thus, it could be argued that magnetic susceptibility can easily result in "false positives," unless all of that 51% genuinely represents cryptotephra horizons. However, much of the sediment between the VVU layers is not characterised by peaks, and many of peaks outside the VVU layers are actually the tails of higher peaks from VVU layers, particularly at the upper stratigraphic boundary. This is most likely due to post-depositional spreading of volcanic clasts into the surrounding sediment by bioturbation. Nevertheless, discrete peaks in magnetic susceptibility which are not contiguous with visible layers should be investigated further, as they may represent departures from normal background MS signal due to the presence of cryptotephras.

*3.1.4. Colour spectrophotometry*

The L* and greyscale curves in Fig. 3 are very similar, but differ slightly from the a* and b* records, which themselves match closely, but appear to be relatively noisier. Negative peaks in L* overlap with 7 out of 9 VVU layers, but the signal noise does not allow clear identification of the layer boundaries (e.g., VVU1). Positive peaks (relative to the background section) are rare in all the spectrophotometric parameters, and do not show any obvious correlation with VVU layers (Table 1). The top of the core trends towards low spectral values, which may reflect a changing consolidation profile. Only 54% of negative peak values overlap with a VVU band (Table 1), suggesting that this technique is not a reliable identifier of discrete volcaniclastic layers when considered in isolation, but it may help with interpretation of the magnetic susceptibility and core-scanning data. The efficiency of the technique may be improved by extending the measurements to higher wavelengths (that are capable of yielding specific mineral reflectance spectra; Clark, 1999), and higher spatial resolution, but this would increase the time required for the measurement and would require a more powerful light source.

*3.1.5. X-radiography*

The results of the X-radiography are presented as an X-ray image of the core (Fig. 3). The sampling resolution is good, it is non-destructive and it can be used as a proxy for density changes in the core, which may indicate the presence of volcanic ash. However, different components of tephra (e.g., vesicular pumice versus dense crystals) yield both negative and positive deviations in the X-ray transparency of the core relative to the background section. In addition, the technique is susceptible to the presence of cracks and other coring artefacts, so that overall the X-radiography images provide an equivocal signal.

*3.1.6. XRF core scanning*

Of the data available from XRF core scanning, ln(Fe/Ca) and ln(Mn/Ca) ratios and the (Fe + Mn)/(Ca + Sr) ratio were found to be the most successful at identifying VVU layers (Fig. 4). Interpretation of the signals is, however, challenging for several reasons. Firstly, as noted above, these parameters may vary as a function of grain-size and/or slight variations in the scanner-sample distance. These variations mean that for some parameters a large proportion of the signal forms significant deviations from the background section that do not appear to be related to the presence of tephra. Hence, both positive and negative peaks overlap with the VVU layers, and in some cases within the same VVU layer. Different volcaniclastic layers and parameters also record different signals (Fig. 4). For example, layer VVU7 yields a strong, but narrow Fe/Ca peak, whereas the signal for Mn/Sr and Mn/Ca is broader. Some of these patterns may be related to post-depositional

**Table 1**
Peaks refer to values exceeding the lower or upper defined limits (termed negative and positive peaks respectively) highlighted in Figs. 2, 3 and 4 with orange lines. Signal refers to all the measurements for a particular technique. If multiple indices are measured for one technique, the one used in this table is highlighted in bold (e.g. **L*** for colour spectrophotometry).

| Technique | | % Visual tephras (VT) detected/total VTs | Total % of peaks | % Proportion of peaks to signal in VT bands | % Peaks occurring in a VT band[a] | Benefits | Limitations |
|---|---|---|---|---|---|---|---|
| Component analysis/point counting (**non-vesicular juvenile clasts**) Positive peaks | | 5/9 = 56% | 34% | 61% | 71% | Provides important characterisation information | Poor resolution and very slow, destructive, dilution effects, noisy signal due to difficulty in defining background values |
| Grain-size (**% >63 μm**) Positive peaks | | 5/9 = 56% | 26% | 50% | 68% | Cost effective, provides sedimentological information, e.g. grading and sorting | Tephra layers can be both fine and coarse grained, so not definitive; poor resolution, fairly slow and destructive |
| Magnetic susceptibility Positive peaks | | 8/9 = 89% | 67% | 92% | 49% | Fast and cost effective, non-destructive, sampling resolution is fairly good. | Sub cm tephra fallout layers may be missed. |
| Colour spectrophotometry (**L***) | Positive peaks | 2/9 = 22% | 1.4% | 0.8% | 20% | Fast and cost effective, non-destructive, sampling resolution is fairly good | Signal is quite ambiguous. Tephra layers can display a range of different colour and lightness properties. |
| | Negative peaks | 7/9 = 78% | 46% | 69% | 54% | Can provide image sedimentary structures, non-destructive, fast, provides down core density changes, excellent sampling resolution | Information is qualitative and difficult to interpret, very sensitive to cracks and other core artefacts. |
| X-radiography | | N/A | N/A | N/A | N/A | | |
| XRF core scanning **ln(Fe/Ca)**, **ln(Mn/Ca)**, **Fe + Mn/Ca + Sr** | Positive peaks | 7/8 = 88% | 23%, 9.5%, 22% | 50%, 20%, 50% | 75%, 73%, 80% | Can provide relative chemical information, excellent sampling resolution, fast, non-destructive | Semi-quantitative chemistry, costly, grain size and water content can have major impacts |
| | Negative peaks | 6/8 = 75% | 38%, 28%, 43% | 23%, 15%, 27% | 21%, 18%, 22% | | |

[a] Remaining percentage could reflect presence of cryptotephras/or poorly-defined VT boundaries (see Fig. 5).

diagenesis, such as Mn reduction and diffusion as a result of low pore water oxygen concentrations associated with ash deposition (Hembury et al., 2012), but it is important to recognise that the XRF data are semi-quantitative and strongly dependent on grain characteristics.

Despite these caveats, positive peaks in the elemental ratios provided by XRF core scanning were successful in identifying the VVU layers, such that 73–80% of peak values (for ln(Fe/Ca), ln(Mn/Ca) and (Fe + Mn)/(Ca + Sr)) lie within the VVU layers (Table 1). Positive peaks in ln(Fe/Ca) showed some overlap with 7 out of 8 VVU layers within the range scanned (the first 70 cm was not scanned, and therefore did not cover the first visible volcaniclastic unit, VVU1), but the signal is weak, with only a small proportion of the total thickness of the VVU layers (22–53%) coinciding with a positive peak. This suggests that XRF core scanning has difficulty in defining layer thicknesses and in identifying cryptotephras in settings where volcanic grains are present in the background sediment, but that it may be more successful where the background sediment is dominated by a single, non-volcanogenic, sediment component. It should be noted that down core variation in chemical composition may also occur as a result of the changes in the regional marine conditions, which may bring fluxes of different sediment types. However, this effect is negligible for the region around Montserrat within this time range.

### 3.2. Identifying cryptotephras

From the range of analytical techniques described above, the following methods appear to have the most potential for detecting cryptotephras: magnetic susceptibility, negative peaks of L*, and positive peaks in ln(Fe/Ca) and ln(Mn/Ca) (Fig. 5). It is important to note, however, that none of these techniques produce peaks that overlap with all the VVU layers. Thus, there is no single parameter that appears to uniquely define the presence or absence of discrete volcaniclastic layers in the sediment core. As a working hypothesis, therefore, the potential presence of a cryptotephra is posited when two or more of the techniques display peaks at the same stratigraphic level, outside the depth range occupied by the VVU layers (red bands in Fig. 5). If these peaks are contiguous with an overlying or underlying VVU layer, however, they may be taken to reflect spreading of the signal due to diagenesis, bioturbation, or coring artefacts (such as smearing). Exclusion of these contiguous peaks leaves six potential cryptotephras (highlighted by the star symbols in Fig. 5), which have been sampled for further analysis.

### 3.3. Distinguishing tephra fallout deposits from other volcaniclastic material using image analysis

Once a volcaniclastic deposit has been identified in a sediment core, whether by visual logging or other techniques, it is important to distinguish tephra fallout deposits from other volcaniclastic deposits, which are generally transported as gravitational flows. The latter may, for example, be derived from primary volcanic events (i.e. pyroclastic-density-currents) or result from secondary reworking of volcanic material (e.g., turbidites derived from lahars, landslides or floods).

The distinct transport processes producing gravitational-flow deposits will likely yield distinct grain morphologies relative to tephra fallout deposits, and an identification technique based on grain-scale image analysis has therefore been tested using microscope photographs of the 9 VVU layers and 6 non-visible volcaniclastic accumulations (potential cryptotephras). To calibrate the method, samples were analysed from known tephra-fallout deposits and known volcaniclastic deposits of other origins, highlighted in Fig. 1 (a volcaniclastic turbidite, a mixed bioclastic-volcaniclastic turbidite, a subaerial lahar deposit and a subaerial pyroclastic density current deposit). The turbidites were sampled from cores collected more proximal to Montserrat (volcanic clasts from the 8–12 ka Lower Volcaniclastic and Bioclastic Unit (Cassidy et al., 2013); Fig. 1); and a scoria- and pumice-bearing turbidite derived from the South Soufrière Hills (Lower SSH Unit; Cassidy et al., 2014);

Fig. 1). The turbidites show clear evidence from sedimentology, lithology and geochemistry of a reworked origin. The lahar sample is from the Belham valley on Montserrat, which transports recently erupted material during heavy rains (Fig. 1). The pyroclastic density current deposit is from a subaerial exposure in the Trants area of Montserrat, and formed from the most recent dome collapse of Soufrière Hills in 2010 (Fig. 1). The tephra-fallout deposits were collected in trays by the Montserrat Volcano Observatory during individual eruptions dating from 1996 to 2010 (Fig. 1).

Average values for perimeter length, area and aspect ratio were determined from ~300 clasts for each sample. The aspect ratio/area and perimeter length/area values show clear distinctions between the tephra-fallout deposits and other volcaniclastic deposits (Fig. 6). The aspect ratio/area index relates to both the elongation of the clasts and their regularity. The value of this index is generally higher (more elongate and irregular) for the fallout deposits, as clasts in these deposits have been less subject to processes such as comminution, saltation and attrition relative to the other volcaniclastic deposits, which experience high energy, erosive, transport (e.g., Manga et al., 2011). Similarly, the perimeter/area index equates closely with the angularity of the clasts, and is again generally higher for tephra fallout clasts due to the same transport-related processes.

The sorting index, based on the standard deviation of clast areas using the Folk and Ward (1957) method (geometric) can also be determined. Measurement of the sorting index via image analysis techniques has the advantage over conventional grain-size analyses in that these parameters can be measured on much smaller quantities of separated clasts. Lower sorting index values indicate better sorting, with tephra fallout deposits typically being moderately- to well-sorted (Walker et al., 1971; Sparks et al., 1997). Volcaniclastic flow deposits, whether primary or secondary, are generally less well-sorted, as the material is emplaced more quickly (Sigurdsson et al., 1980; Carey and Sigurdsson, 1984; Fisher and Schmincke, 1994), with the caveat that some turbidite deposits become well-sorted during gradual sedimentation (Kneller and Buckee, 2000; Mulder and Alexander, 2001). This latter process is evidenced by the range of sorting index values found throughout the turbidite deposits (shown by the red and blue arrows in Fig. 6; Cassidy et al., 2013, 2014).

The known volcaniclastic and tephra fallout deposits fall in two clearly separate fields in Fig. 6, using the parameters above. When data from the VVU and potential cryptotephra deposits from JC18-19 are included on the same plot, only 4 of the 9 VVU layers, and 4 of the 6 potential cryptotephras fall within the field defined by the known tephra fallout deposits. The other deposits are volcaniclastic, but they appear to have been deposited by processes other than atmospheric fallout. Thus, the image-analysis method appears to provide a relatively rapid and consistent approach for categorising tephra deposits. It does, however, require further testing with a range of tephra compositions and explosive eruption styles. For example, some fallout deposits may fall outside the defined field in Fig. 6 if they are poorly-sorted as a result of ash transportation at different levels in the atmosphere with differing wind trajectories, as in the 1991 Pinatubo eruption (Wiesner et al.,

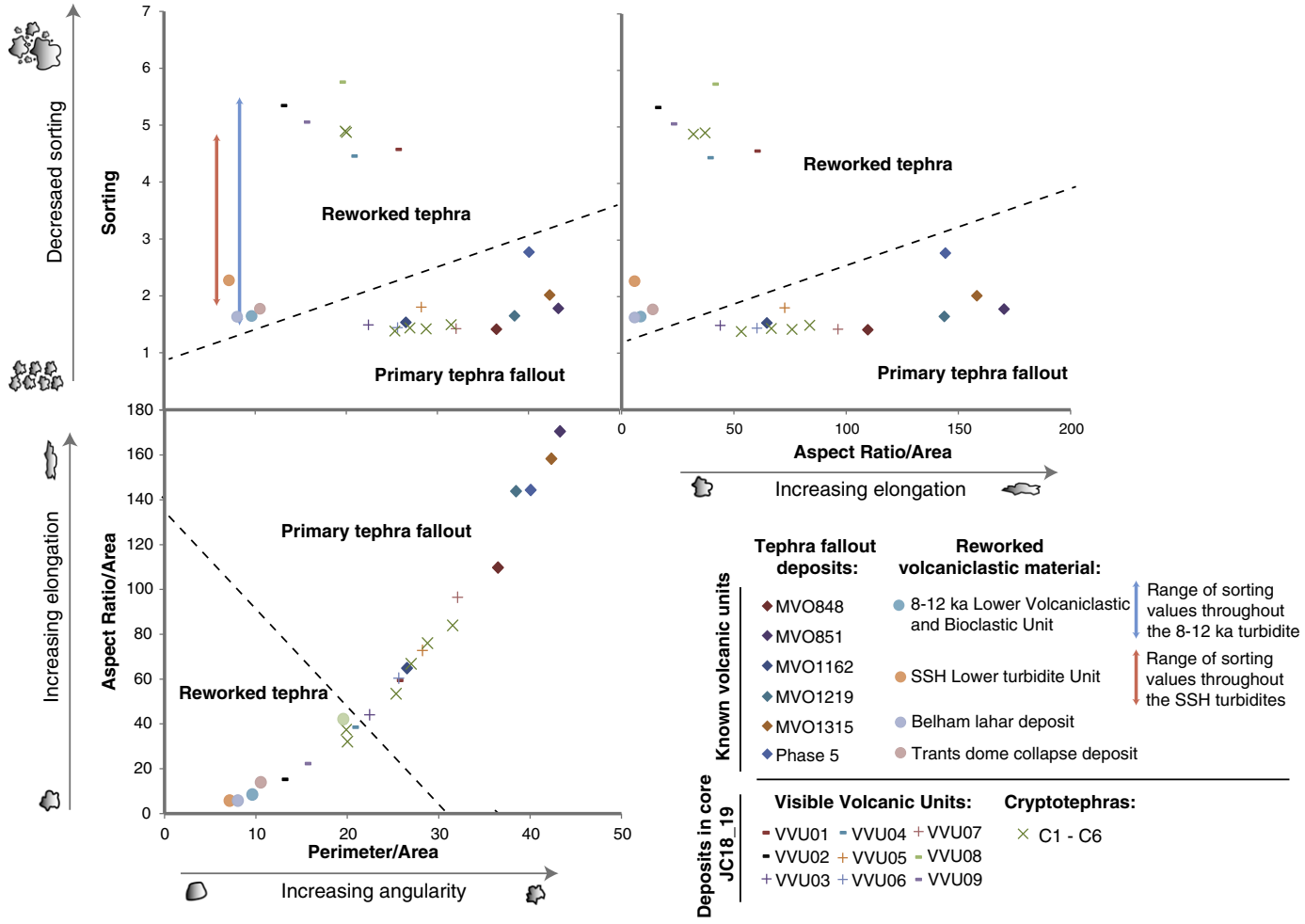


**Fig. 6.** Three parameters: aspect ratio/area, perimeter/area and sorting are used to distinguish tephra fallout deposits from other volcaniclastic deposits. This method is calibrated using known tephra fallout deposits from recent eruptions on Montserrat and known reworked and volcaniclastic flow deposits. Crossed symbols denote those VVUs that fall within the primary tephra fallout group using this image analysis method.

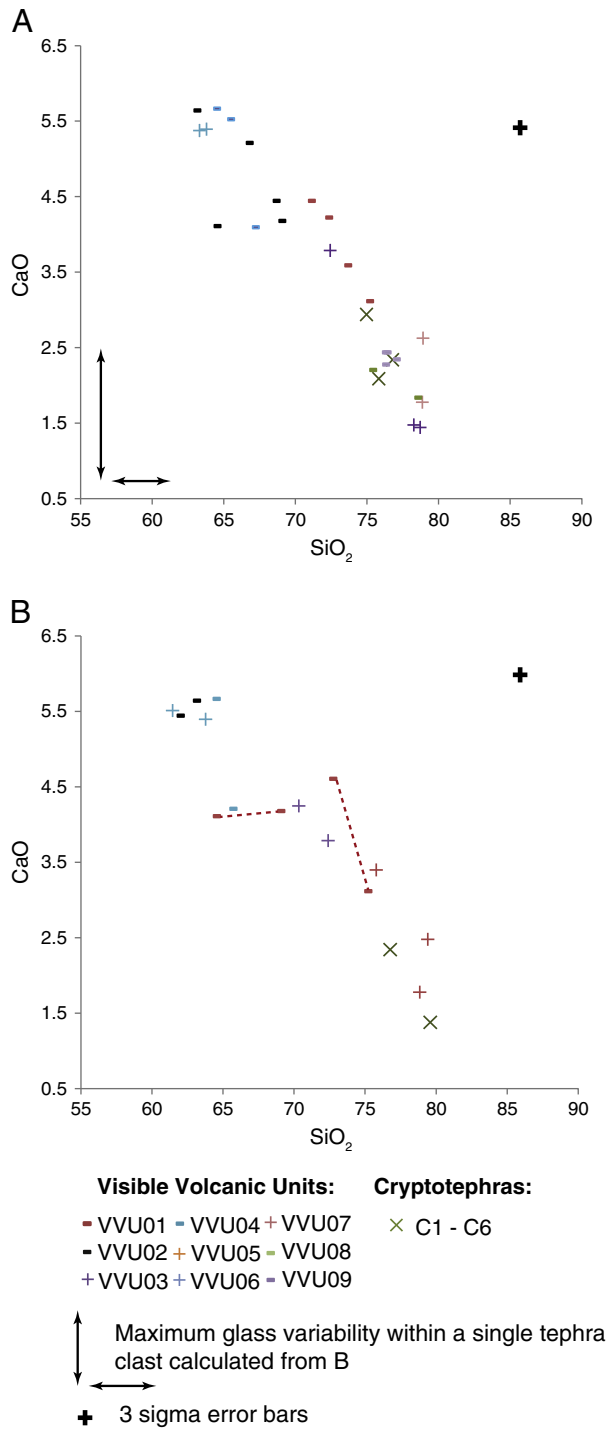


**Fig. 7.** A) Glass geochemistry plot of the different volcaniclastic units sampled. The symbols are the same as used in Fig. 6. The crossed symbols denote those VVUs that fall within the primary tephra fallout group using the image analysis method in Fig. 6. All values are normalised to 100% anhydrous. The data points plotted are averages from multiple analyses from a single grain. B) Shows the variation in chemistry within a single tephra clast. This variation is illustrated using arrows in Fig. 7A. Where inter-glass variability was measured for two glass clasts within one sample (e.g. VVU 2), dashed tie lines are used to show measurements made on the same clast. Error quoted.

2004). Furthermore, aggregation of clasts of varying sizes commonly occurs in plumes from large explosive eruptions, leading to less well-sorted fallout deposits, which are commonly bimodal and contain a fine ash mode derived from aggregation (Carey and Sigurdsson, 1982; Rose and Durant, 2011; Stevenson et al., 2012; Brown et al., 2012). For the volcaniclastic deposits deemed as non-tephra-fallout deposits, this does not necessarily preclude the presence of some primary tephra-fallout grains as these are average values, and the comminution processes occurring in co-ignimbrite plumes, for example, may plot outside our defined tephra-fallout field. Nevertheless, in this study, the clear division between the two fields suggests that this is a potentially powerful method in tephrochronology studies.

Once the volcaniclastic units have been identified and categorised using the indices described above, destructive geochemical analyses can then be used to obtain further information (e.g. determining the origin of tephra layers, correlating layers between sites, studying the evolution of a single volcano, etc.). Importantly, these studies can be undertaken in the confidence that the tephra deposit under consideration is of clear primary origin.

### *3.4. Distinguishing tephra fallout deposits from other volcaniclastic material using glass geochemistry*

Multiple studies utilise glass geochemistry to distinguish primary from reworked volcanic deposits, based on the amount of inter-clast chemical variability within one sample (Schneider et al., 2001; Kutterolf et al., 2009; Lowe, 2011; Schindlbeck et al., 2013). The premise of this hypothesis is that a large compositional scatter between clasts indicates clast origins from multiple volcanic events, and the deposit is therefore reworked. Conversely, a tight cluster of data in geochemical space suggests a primary volcanic origin. However, it should be noted that both lahar and PDC-derived deposits could be dominated by material produced during a single eruption, and thus form compositionally homogeneous deposits. Additionally, not all large explosive eruptions are compositionally homogeneous, but may erupt glass compositions across a wide compositional range (e.g. Kratzmann et al., 2009).

The purpose of using glass chemistry in this paper is to assess how effectively it can discriminate reworked from primary eruption deposits. Fig. 7A uses a $SiO_2$ vs. CaO plot to illustrate this method in the same manner as used in other studies (Lowe, 2011). Fig. 7A shows that glass chemistry alone is not useful for achieving the objectives listed above. In general, the glass chemistry from all our units displays a surprising lack of intra-unit heterogeneity, and is thus an ambiguous tool for discriminating fallout deposits from other volcaniclastic deposits. This is because, as noted above, events such as lahars may sample material that is relatively homogeneous in composition (cf. VVU 9). This may be particularly true for small events, which may sample only a limited portion of volcaniclastic material (e.g. a dome collapse-derived landslide). When compared to the image analysis method in Fig. 6, there is a broad pattern of greater variability in glass compositions for the non-fallout deposits (based on these limited data). However, there are problems with the using glass chemistry alone to ascertain the origin of a volcaniclastic deposit. Such problems are as follows:

(1) There are no objective rules for defining how much chemical variation constitutes a compositionally homogeneous cluster, and this makes this method ambiguous and subjective.
(2) Even if clear criteria for compositional homogeneity can be defined, homogeneous deposits may be formed from a variety of non-fallout processes (e.g. lahars). Conversely, some explosive eruption fallout deposits are strongly bimodal, or have a dispersed compositional field (e.g. the eruption of Cerro Hudson in 1991, cf. Kratzmann et al., 2009).
(3) There may be considerable variability in the glass composition within a single clast, as shown in Fig. 7B. This indicates the minimum compositional spread within any deposit, which may be relatively broad (Fig. 7A). A large number of analyses are therefore required to rigorously define the compositional field characterising a particular deposit.
(4) An inherent weakness of this approach is that it only analyses glassy, vesicular clasts. Within mixed deposits, such clasts may

give a false impression of relative homogeneity. For example, a bioclastic turbidite that contained no pumice derived from its source region, but did erode a previously deposited pumice fall deposit during transport, would appear as a homogeneous fall deposit by this technique, if the pumice was selectively picked out for analysis without taking into account the mixed nature of the other clast types within the unit (c.f. VVU 9).

(5) Tephra clasts often have a large proportion of microlites in the matrix; in the case of the Soufriere Hills ~95% of the groundmass is comprised of microlites; (Sparks et al., 2000). This makes it difficult to probe the glass without having interference from these microlite phases. This effect meant that over 50% of the data points collected in this study had to be rejected, resulting in the small quantity of data in Fig. 7A. This is a common feature of many pyroclastic rocks, particularly those that are relatively mafic and/or derived from less explosive modes of fragmentation.

(6) Many volcanoes have a monotonous eruption composition over several eruptions (as is the case for the Soufriere Hills; Christopher et al., 2014). Thus, if a turbidite contains volcanic material from multiple different eruptions of similar composition, glass chemistry alone may not distinguish it from a deposit produced by a single volcanic event.

In addition to the above, obtaining electron microprobe data can be expensive and laborious. As our points show, glass chemistry alone is not a good indicator of the origin of a volcaniclastic deposit, but must be used with other methods and lines of evidence. This method should not be discounted as it has been used with some success in different volcanic settings to this study, especially when supported by sedimentological and petrological lines of evidence (c.f. Brendryen et al., 2010; Albert et al., 2012). Nonetheless, we suggest that the array of other techniques described here provides a more objective means of interpreting the origin of a volcaniclastic deposit. Once these techniques have been used to identify tephra fallout deposits, glass chemistry is then a powerful tool, along with other chemical (e.g. crystal compositions) and stratigraphic data, for correlating these deposits between cores.

### 3.5. Nature of volcanic activity

The nature of the source volcanic activity responsible for primary volcaniclastic deposits is difficult to discern based solely on microscope observations of samples taken from a core. Further inferences may be made based on the thickness of the deposit, the average clast size and the type of clasts present. For example, a high proportion of vesicular clasts might suggest an explosive "open-vent" eruption, whereas dominance of non-vesicular clasts may suggest an explosive event associated with collapse of a lava dome (closed-vent eruption). In contrast, glass shards and crystal fragments are ubiquitous throughout most of the deposits and the background sediment, and thus appear to be common to many eruption types.

## 4. Summary of core interpretation techniques

The first step in the search for cryptotephras and in the discrimination of tephra fallout deposits from other volcaniclastic deposits should ideally involve the use of fast, non-destructive and high-spatial resolution techniques. Of the techniques employed here, sedimentary logging, XRF-core scanning, magnetic susceptibility and colour spectrophotometry all fall into these categories. Of these techniques, XRF-core scanning was found to be the most sensitive to identifying volcaniclastic accumulations, but potentially weak for identifying cryptotephras and accurately recording deposit thicknesses, for which magnetic susceptibility was more powerful. Magnetic susceptibility measurements are less sensitive than XRF-core scanning, but are more reliable in detecting tephra layers. In general, the more techniques that are used, the more likely it is that an unequivocal volcaniclastic signal will be obtained. Fortunately, several of these techniques can be run in parallel using multi-sensor instruments. The results of this study suggest that a positive signal from at least two independent techniques is required to detect the possible presence of diffuse cryptotephras in marine sediment cores. It is important to recognise, however, that core scanning techniques only aid detection of zones of volcaniclastic sediment accumulation, and further investigation by direct sampling is required to determine the nature of the identified deposit, and whether it truly represents a cryptotephra derived from a fallout deposit.

Component analysis and study of grain size variations are not appropriate for whole-core analysis in the way used in this study because they are time-intensive and destructive. In addition, they do not readily identify discrete tephra layers in environments where the background sediments also contain volcanic clasts. Nevertheless, they provide critical information when focussing on specific horizons identified by visual logging and the non-destructive techniques outlined above. Hence, component and grain size analyses should take place after using the automated techniques. In addition more advanced practices, such as use of a polarising microscope and automatic point counter coupled with in-situ glass chemistry, although time-consuming, may be necessary (Schindlbeck et al., 2013). It is important to note that other techniques may be more useful in detecting cryptotephras in other settings. For example, Gudmundsdóttir et al. (2011) were successful in applying component analysis and grain size changes to detect cryptotephras in marine sediment cores from the North Icelandic shelf, owing to the fine grain size of the background sediment and low quantity of background volcaniclastic material. In settings such as Lesser Antilles (i.e. volcanic arcs), where the background sediment contains volcaniclastic sediment, identifying cryptotephras is more challenging, and component and grain-size analyses are of limited value.

The core analysis protocol described in this paper yields fast results and makes efficient use of limited core material. Image analysis of the separated volcaniclastic material then provides a powerful and objective means of determining the nature of a volcaniclastic deposit (i.e., primary fallout versus flow transport) from granulometric measurements (e.g., grain-size, sorting) in thin and/or diffuse volcaniclastic layers.

Fig. 8 represents the results of this study, demonstrating the presence both of cryptotephras and visible volcanic units in the core and how these units can equally be derived from a primary tephra fallout event or may represent areas of reworked volcaniclastic sediment. Indeed, 6 out of the 15 volcaniclastic units identified in this study are interpreted as non-fallout deposits. When Le Friant et al. (2008) examined the eruptive history of Montserrat, the authors postulated that all the deposits discovered in their core (Carmon 2; Fig. 1) represented primary tephra fallout units. However, evidence from this study on a core located just 8 km away from Carmon 2 (Fig. 1) suggests that there is a significant contribution of volcaniclastic material deposited via other processes.

## 5. Conclusions

Various methods have been tested for detecting tephra/volcaniclastic units and cryptotephras in marine sediment cores. Their success was judged initially on how well they could detect visually identified volcaniclastic units in a test core off the volcanic island of Montserrat. This analysis indicates that sedimentary logging, XRF core scanning and magnetic susceptibility most clearly identify volcaniclastic accumulations, but their efficacy increases when they are used in conjunction with other non-destructive scanning techniques, such as colour spectrophotometry. Image analysis of volcaniclastic grains subsequently separated from targeted horizons can then be used to provide rapid and objective discrimination of primary tephra fallout layers from other volcaniclastic (often reworked) deposits using indices representing the degree of angularity, elongation and sorting of the grains.

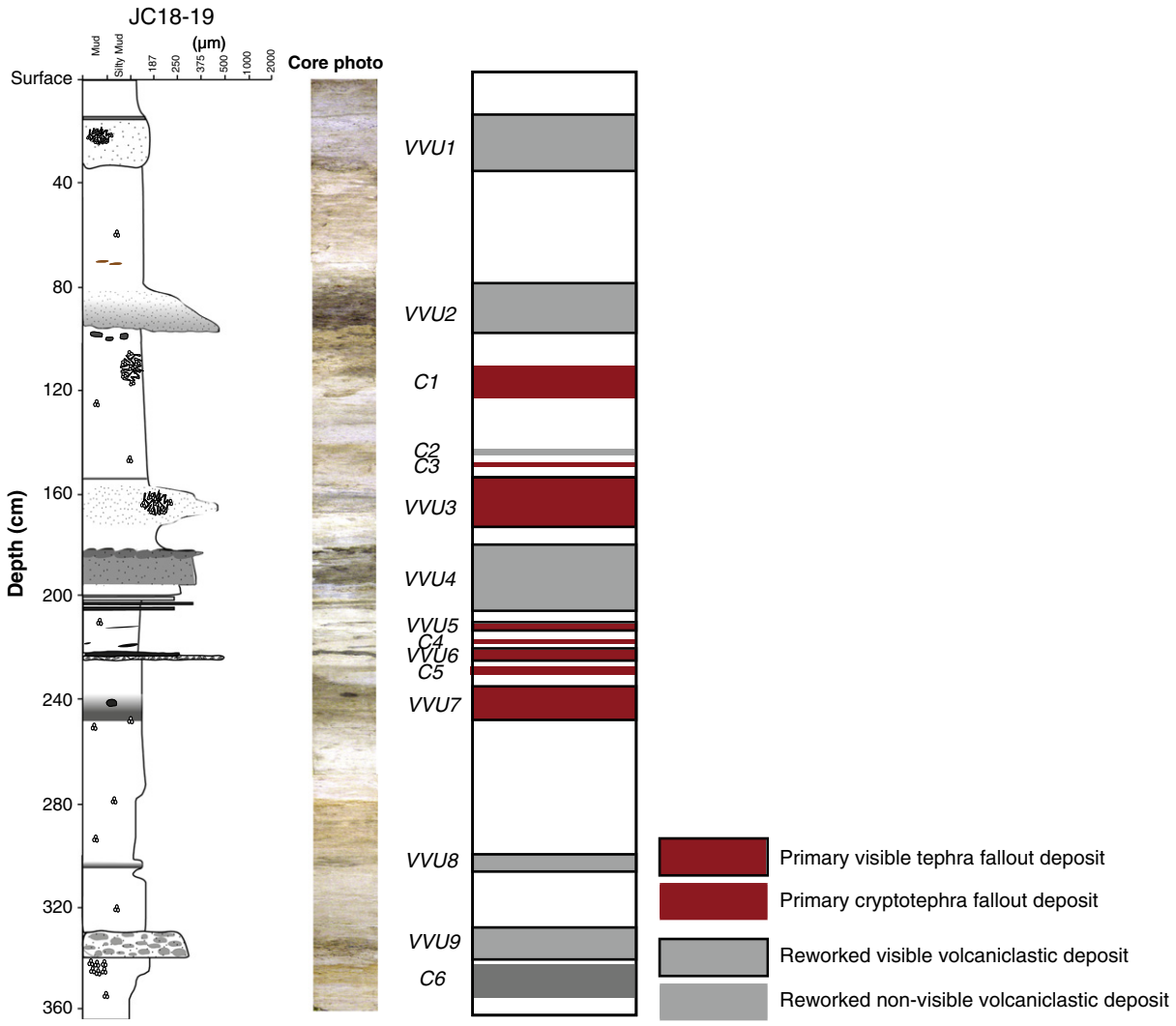


**Fig. 8.** Summary figure highlighting the visible and non-visible/cryptotephras units which have been deemed as either tephras fallout deposits or instead represent volcaniclastic flow deposits. Depth in cm is the depth below the seafloor.

As a result of these studies the following protocol is suggested for the fast and efficient detection of tephra fallout deposits in marine sediment cores:

(1) Construct a graphic log of the core, taking into consideration sedimentary and visual features, to create a record of the visible volcaniclastic units
(2) Use fast, non-destructive, core scanning techniques (e.g. XRF core scanning, magnetic susceptibility, colour reflectance) to generate high spatial resolution, down-core records
(3) From these records, select a depth interval of background hemipelagic sediment that shows minimal variation in the various recorded data
(4) Assign "tephra detection limits" for each technique by averaging the data over the background interval and adding/subtracting twice the standard deviation of the mean. This removes the background "noise" signal and anything exceeding these limits provides a legitimate target for further testing
(5) After target horizons have been identified, they should be sampled and photographed under a microscope for image analysis in order to distinguish primary tephra fallout deposits from other volcaniclastic deposits on the basis of perimeter/area (angularity), aspect ratio/area (elongation) and grain size variation (sorting)
(6) Further analyses (e.g. specific geochemical and dating procedures) can then be undertaken in the confidence that the samples under considerations are primary fallout deposits.

## Acknowledgements

Laboratory assistance was provided by Guy Rothwell and Belinder Aker. This work was helped by discussions with Jon Davidson, John Stevenson, Steve Roberts and Tom Gernon. Many thanks go to the crew and scientist onboard the JC18 and Steve Sparks is thanked for use of the JCR123 sediment cores. This work was partly funded by a NERC studentship; M.C. and S.W. thank NERC for financial support, via grant NE/K000403/1. Steffen Kutterolf and an anonymous reviewer are thanked for their constructive reviews, which helped improve this article.

## References

Abbott, P.M., Davies, S.M., Austin, W.E.N., Pearce, N.J.G., Hibbert, F.D., 2011. Identification of cryptotephra horizons in a North East Atlantic marine record spanning marine isotope stages 4 and 5a (similar to 60,000–82,000 a b2k). Quat. Int. 246, 177–189.
Albert, P.G., Tomlinson, E.L., Smith, V.C., Di Roberto, A., Todman, A., Rosi, M., Marani, M., Muller, W., Menzies, M.A., 2012. Marine-continental tephra correlations: volcanic glass geochemistry from the Marsili Basin and the Aeolian Islands, Southern Tyrrhenian Sea, Italy. J. Volcanol. Geotherm. Res. 229–230, 74–94.

Allen, J.R.L., 1971. Instantaneous sediment deposition rates deduced from climbing-ripple cross-lamination. J. Geol. Soc. London 127, 553–561.

Allen, J.R.L., Brandt, U., Brauer, A., Hubberten, H.-W., Huntley, B., Keller, J., Kraml, M., Mackensen, A., Mingram, J., Jörg, F.W., et al., 1999. Rapid environmental changes in southern Europe during the last glacial period. Nature 400, 740–743.

Amy, L.A., Talling, P.J., 2006. Anatomy of turbidites and linked debrites based on long distance (120 × 30 km) bed correlation, Marnoso Arenacea Formation, Northern Apennines, Italy. Sedimentology 53 (1), 161–212.

Barclay, J., Rutherford, M.J., Carroll, M.R., Murphy, M.D., Devine, J.D., Gardner, J., Sparks, R. S.J., 1998. Experimental phase equilibria constraints on pre-eruptive storage conditions of the Soufrière Hills magma. Geophys. Res. Lett. 25 (18), 3437–3440.

Bertrand, S., Castiaux, J., Juvigné, E., 2008. Tephrostratigraphy of the late glacial and Holocene sediments of Puyehue Lake (Southern Volcanic Zone, Chile, 40°S). Quat. Res. 70, 343–357.

Blockley, S.P.E., Pyne-O'Donnell, S.D.F., Lowe, J.J., Matthews, I.P., Stone, A., Pollard, A.M., Turney, C.S.M., Molyneux, E.G., 2005. A new and less destructive laboratory procedure for the physical separation of distal glass tephra shards from sediments. Quat. Sci. Rev. 24, 1952–1960.

Blott, S.J., Pye, K., 2001. GRADISTAT: a grain size distribution and statistics package for the analysis of unconsolidated sediments. Earth Surf. Process. Landf. 26 (11), 1237–1248.

Blum, P., 1997. Physical properties handbook: a guide to the ship board measurement of physical properties of deep-sea cores. ODP Tech. Note 26. Ocean Drilling Program College Station, Tex.

Bond, G., Heinrich, H., Broecker, W., Labeyrie, L., McManus, J., Andrews, J., Huon, S., Jantschik, R., Clasen, S., Simet, C., Tedesco, K., Klas, M., Bonani, G., Ivy, S., 1992. Evidence for massive discharges of icebergs into the North Atlantic ocean during the last glacial period. Nature 360 (6401), 245–249.

Bouma, A.H., 1962. Sedimentology of Some Flysch Deposits: A Graphic Approach to Facies Interpretation. Elsevier, Amsterdam, (168 pp.).

Bourne, A.J., Lowe, J.J., Trincardi, F., Asioli, A., Blockley, S.P.E., Wulf, S., Matthews, I.P., Piva, A., Vigliotti, L., 2010. Distal tephra record for the last ca 105,000 years from core PRAD 1–2 in the central Adriatic Sea: implications for marine tephrostratigraphy. Quat. Sci. Rev. 29, 3079–3094.

Boygle, J., 1999. Variability of tephra in lake and catchment sediments, Svínavatn, Iceland. Glob. Planet. Chang. 21, 129–149.

Brendryen, J., Haflidason, H., Sejrup, H.P., 2010. Norwegian Sea tephrostratigraphy of marine isotope stages 4 and 5: prospects and problems for tephrochronology in the North Atlantic region. Quat. Sci. Rev. 29 (7–8), 847–864.

Brown, R.J., Bonadonna, C., Durant, A.J., 2012. A review of volcanic ash aggregation. Phys. Chem. Earth Parts A/B/C.

Bryn, P., Berg, K., Forsberg, C.F., Solheim, A., Kvalstad, T.J., 2005. Explaining the Storegga Slide. Mar. Pet. Geol. 22 (1–2), 11–19.

Calder, E.S., Cole, P.D., Dade, W.B., Druitt, T.H., Hoblitt, R.P., Huppert, H.E., Ritchie, L., Sparks, R.S.J., Young, S.R., 1999. Mobility of pyroclastic flows and surges at the Soufrière Hills Volcano, Montserrat. Geophys. Res. Lett. 26 (5), 537–540.

Carel, M., Siani, G., Delpech, G., 2011. Tephrostratigraphy of a deep-sea sediment sequence off the south Chilean margin: new insight into the Hudson volcanic activity since the last glacial period. J. Volcanol. Geotherm. Res. 208 (3–4), 99–111.

Carey, S., 1997. Influence of convective sedimentation on the formation of widespread tephra fall layers in the deep sea. Geology 25 (9), 839–842.

Carey, S., 2000. Volcaniclastic sedimentation around island arc. In: Sigurdsson, H. (Ed.), Encyclopedia of Volcanoes. Academic press, pp. 627–642.

Carey, S.N., Sigurdsson, H., 1982. Influence of particle aggregation on deposition of distal tephra from the May 18, 1980, eruption of Mount St. Helens volcano. J. Geophys. Res. 87 (NB8), 7061–7072.

Carey, S.N., Sigurdsson, H., 1984. A model of volcanogenic sedimentation in marginal basins Marginal Basin Geology. In: Kokelaar, B.P., Howells, M.F. (Eds.), Volcanic and Associated Sedimentary and Tectonic Processes in Modern and Ancient Marginal Basins. Journal of the Geological Society London Special Publication. 16.

Cas, R.A.F., Wright, J.V. (Eds.), 1987. Volcanic Successions. Chapman & Hall, London (528 pp.).

Caseldine, C., Baker, A., Barnes, W.L., 1999. A rapid, non-destructive scanning method for detecting distal tephra layers in peats. The Holocene 9 (5), 635–638.

Cassidy, M., Taylor, R.N., Palmer, M.R., Cooper, R.J., Stenlake, C., Trofimovs, J., 2012. Tracking the magmatic evolution of island arc volcanism: insights from a high-precision Pb isotope record of Montserrat, Lesser Antilles. Geochem. Geophys. Geosyst. 13.

Cassidy, M., T. J., Palmer, M.R., Talling, P.J., Watt, S.F.L., Moreton, S.G., Taylor, R.N., 2013. Timing and emplacement dynamics of newly recognised mass flow deposits at similar to 8–12 ka offshore Soufrière Hills volcano, Montserrat: how submarine stratigraphy can complement subaerial eruption histories. J. Volcanol. Geotherm. Res. 253, 1–14.

Cassidy, M., Trofimovs, J., Watt, S.F.L., Palmer, M.R., Taylor, R.N., Gernon, T.M., Talling, P.J., Le Friant, A., 2014. Multi-stage collapse events in the South Soufrière Hills, Montserrat, as recorded in marine sediment cores. In: Wadge, G., Robertson, R., Voight, B. (Eds.), The Eruption of Soufrière Hills Volcano, Montserrat from 2000 to 2010. Memoir of the Geological Society, London.

Christopher, T., Humphreys, M.C.S., Genareau, K., Henton, S., Donovan, A., Barclay, J., Plail, M. (Eds.), 2014. Petrological and geochemical overview of the Soufriere Hills eruption (1995–2010). Wadge, G., Robertson, R., Voight, B. (Eds.), 2014. The Eruption of Soufriere Hills Montserrat from 2000 to 2010: The Geological Society of London.

Clark, R.N., 1999. Chapter 1: spectroscopy of rocks and minerals, and principles of spectroscopy. In: Rencz, R.N. (Ed.), Manual of Remote Sensing, Remote Sensing for the Earth Sciences. John Wiley and Sons, New York, pp. 3–58.

Cole, P.D., Calder, E.S., Druitt, T.H., Hoblitt, R., Robertson, R., Sparks, R.S.J., Young, S.R., 1998. Pyroclastic flows generated by gravitational instability of the 1996–97 lava dome of Soufrière Hills Volcano, Montserrat. Geophys. Res. Lett. 25 (18), 3425–3428.

Couch, S., Sparks, R.S.J., Carroll, M.R., 2001. Mineral disequilibrium in lavas explained by convective self-mixing in open magma chambers. Nature 411 (6841), 1037–1039.

Couch, S., Sparks, R.S.J., Carroll, M.R., 2003. The kinetics of degassing-induced crystallization at Soufrière Hills volcano, Montserrat. J. Petrol. 44 (8), 1477–1502.

Croudace, I.W., Rindby, A., Rothwell, R.G., 2006. ITRAX: description and evaluation of a new multi-function X-ray core scanner. In: Rothwell, R.G. (Ed.), New Techniques in Sediment Core Analysis. The Geological Society of London, pp. 51–63.

Currie, L.A., 1968. Limits for qualitative detection and quantitative determination: application to radiochemistry. Anal. Chem. 40, 586–593.

de Fontaine, C.S., Kaufman, D.S., Anderson, R.S., Werner, A., Waythomas, C.F., Brown, T.A., 2007. Late quaternary distal tephra-fall deposits in lacustrine sediments, Kenai Peninsula, Alaska. Quat. Res. 68 (1), 64–78.

DeMets, C., Jansma, P.E., Mattioli, G.S., Dixon, T.H., Farina, F., Bilham, R., Calais, E., Mann, P., 2000. GPS geodetic constraints on Caribbean-North America plate motion. Geophys. Res. Lett. 27 (3), 437–440.

Dugmore, A.J., Newton, A.J., 1992. Thin tephra layers in peat revealed by X-radiography. J. Archaeol. Sci. 19 (2), 163–170.

Enache, M.D., Cumming, B.F., 2006. The morphological and optical properties of volcanic glass: a tool to assess density-induced vertical migration of tephra in sediment cores. J. Paleolimnol. 35 (3), 661–667.

Engwell, S.L., Sparks, R.S.J., Carey, S.S., 2014. Physical characteristics of tephra layers in the deep sea realm: the Campanian Ignimbrite eruption. In: Austin, W.E.N., Abbott, P.M., Davies, S.M., Pearce, N.J.G., Wastega'rd, S. (Eds.), Marine Tephrochronology. Geol. Soc. Lond. Spec. Publ. 398. http://dx.doi.org/10.1144/SP398.7.

Fine, I.V., Rabinovich, A.B., Bornhold, B.D., Thomson, R.E., Kulikov, E.A., 2005. The Grand Banks landslide-generated tsunami of November 18, 1929: preliminary analysis and numerical modeling. Mar. Geol. 215 (1–2), 45–57.

Volcaniclastic sediment transport and deposition. In: Fisher, R.V., Schmincke, H.U. (Eds.), Sediment Transport and Depositional Processes. Blackwell Scientific Publications (351–388 pp.).

Folk, R.L., Ward, W.C., 1957. Brazos River bar: a studying the significance of grain-size parameters. J. Sed. Petrol. 27, 3–26.

Froggatt, P.C., 1992. Standardization of the chemical analysis of tephra deposits. Report of the ICCT working group. Quat. Int. 13 (14), 93–96.

Froggatt, P.C., Lowe, D.J., 1990. A review of late Quaternary silicic and some other tephra formations from New Zealand: their stratigraphy, nomenclature, distribution, volume, and age. N. Z. J. Geol. Geophys. 33 (1), 89–109.

Turbidites from slope failure on Hawaiian volcanoes. In: Garcia, M.O. (Ed.), Volcano Instability on the Earth and Other Planets. Geol. Soc. Lond. Spec. Publ. 110, pp. 281–294.

Gehrels, M.J., Lowe, D.J., Hazell, Z.J., Newnham, R.M., 2006. A continuous 5300-yr Holocene cryptotephrostratigraphic record from northern New Zealand and implications for tephrochronology and volcanic hazard assessment. The Holocene 16, 173–187.

Gehrels, M.J., Newnham, R.M., Lowe, D.J., Wynne, S., Hazell, Z.J., Caseldine, C., 2008. Towards rapid assay of cryptotephra in peat cores: review and evaluation of various methods. Quat. Int. 178, 68–84.

Gudmundsdóttir, E.R., Eiriksson, J., Larsen, G., 2011. Identification and definition of primary and reworked tephra in Late Glacial and Holocene marine shelf sediments off North Iceland. J. Quat. Sci. 26 (6), 589–602.

Gudmundsdóttir, E.R., Larsen, G., Eiriksson, J., 2012. Tephra stratigraphy on the North Icelandic shelf: extending tephrochronology into marine sediments off North Iceland. Boreas 41 (4), 718–734.

Harford, C.L., Pringle, M.S., Sparks, R.S.J., Young, S.R., 2002. The volcanic evolution of Montserrat using $^{40}Ar/^{39}Ar$ geochronology. In: Druitt, T.H., Kokelaar, B.P. (Eds.), The Eruption of Soufrière Hills Volcano, Montserrat, from 1995 to 1999. Geological Society of London Memoirs, London, pp. 93–113.

Heinrich, H., 1988. Origin and consequences of cyclic ice rafting in the Northeast Atlantic Ocean during the past 130,000 years. Quat. Res. 29 (2), 142–152.

Hembury, D.J., Palmer, M.R., Fones, G.R., Mills, R.A., Marsh, R., Jones, M.T., 2012. Uptake of dissolved oxygen during marine diagenesis of fresh volcanic material. Geochim. Cosmochim. Acta 84, 353–368.

Herd, R.A., Edmonds, M., Bass, V.A., 2005. Catastrophic lava dome failure at Soufrière Hills Volcano, Montserrat, 12–13 July 2003. J. Volcanol. Geotherm. Res. 148 (3–4), 234–252.

Hodgson, D.A., Dyson, C.L., Jones, V.J., Smellie, J.L., 1998. Tephra analysis of sediments from Midge Lake (South Shetland Islands) and Sombre Lake (South Orkney Islands), Antarctica. Antarct. Sci. 10 (1), 13–20.

Houghton, B.F., Wilson, C.J.N., Pyle, D.M., 2000. Pyroclastic fall deposits. In: Sigurdsson, H. (Ed.), Encyclopaedia of Volcanoes. Academic Press, pp. 555–570.

Hunt, J.B., Najman, Y.M.R., 2003. Tephrochronological and tephrostratigraphical potential of Pliocene–Pleistocene volcaniclastic deposits in the Japan Forearc, ODP Leg 186. In: Suyehiro, K., Sacks, I.S., Acton, G.D., Oda, M. (Eds.), Proceedings of the Ocean Drilling Program. Scientific Results, p. 1e29.

Hunt, J.E., Wynn, R.B., Masson, D.G., Talling, P.J., Teagle, D.A.H., 2011. Sedimentological and geochemical evidence for multistage failure of volcanic island landslides: A case study from Icod landslide on north Tenerife, Canary Islands. Geochem. Geophys. Geosyst. 12.

Ilstad, T., Elverhoi, A., Issler, D., Marr, J.G., 2004. Subaqueous debris flow behaviour and its dependence on the sand/clay ratio: a laboratory study using particle tracking. Mar. Geol. 213 (1–4), 415–438.

Juvigné, E., Bertrand, S., Heuschen, B., Tallier, E., 2008. Téphrostratigraphie de sediments lacustres situés en context géodynamique actif: exemple des sediments du lac Icalma (Chili, zone volcanique sud, 38°S). Quaternaire 19, 175–189.

Kandlbauer, J., Carey, S., Sparks, R.S.J., 2013. The 1815 Tambora ash fall: implications for transport and deposition of distal ash on land and the deep sea. Bull. Volcanol. 75 (708).

Kneller, B., Buckee, C., 2000. The structure and fluid mechanics of turbidity currents: a review of some recent studies and their geological implications. Sedimentology 47, 62–94.
Kotaki, A., Katoh, S., Kitani, K., 2011. Correlation of Middle Pleistocene crystal-rich tephra layers from Daisen volcano, southwest Japan, based on the chemical composition and refractive index of mafic minerals. Quat. Int. 246, 105–117.
Kratzmann, D.J., Carey, S., Scasso, R., Naranjo, J.A., 2009. Compositional variations and magma mixing in the 1991 eruptions of Hudson volcano, Chile. Bull. Volcanol. 71 (4), 419–439.
Kuenen, P.H., 1966. Matrix of turbidites: experimental approach. Sedimentology 7, 267–297.
Kutterolf, S., Freundt, A., Perez, W., Moerz, T., Schacht, U., Wehrmann, H., Schmincke, H.U., 2008. Pacific offshore record of plinian arc volcanism in Central America: 1. Along-arc correlations. Geochem. Geophys. Geosyst. 9.
Kutterolf, S., Jegen, M., Mitrovica, J.X., Kwasnitschka, T., Freundt, A., Huybers, P.J., 2013. A detection of Milankovitch frequencies in global volcanic activity. Geology 41 (2), 227–230.
Kylander, M.E., Lind, E.M., Wastegard, S., Lowemark, L., 2012. Recommendations for using XRF core scanning as a tool in tephrochronology. The Holocene 22 (3), 371–375.
Lane, C.S., Blocklye, S.P.E., Mangerud, J., Smith, V.C., Lohne, O.S., Tomlinson, E.L., Matthews, I.P., Lotter, A.F., 2012. Was the 12.1 ka Icelandic Vedde Ash one of a kind? Quat. Sci. Rev. 33, 87–99.
Le Friant, A., Harford, C.L., Deplus, C., Boudon, G., Sparks, R.S.J., Herd, R.A., Komorowski, J.C., 2004. Geomorphological evolution of Montserrat (West Indies): importance of flank collapse and erosional processes. J. Geol. Soc. 161, 147–160.
Le Friant, A., Lock, E.J., Hart, M.B., Boudon, G., Sparks, R.S.J., Leng, M.J., Smart, C.W., Komorowski, J.C., Deplus, C., Fisher, J.K., 2008. Late Pleistocene tephrochronology of marine sediments adjacent to Montserrat, Lesser Antilles volcanic arc. J. Geol. Soc. 165, 279–289.
Le Friant, A., Deplus, C., Boudon, G., Sparks, R.S.J., Trofimovs, J., Talling, P., 2009. Submarine deposition of volcaniclastic material from the 1995–2005 eruptions of Soufrière Hills volcano, Montserrat. J. Geol. Soc. 166, 171–182.
Le Friant, A., Deplus, C., Boudon, G., Feuillet, N., Trofimovs, J., Komorowski, J.C., Sparks, R.S.J., Talling, P., Loughlin, S., Palmer, M., Ryan, G., 2010. Eruption of Soufrière Hills (1995–2009) from an offshore perspective: insights from repeated swath bathymetry surveys. Geophys. Res. Lett. 37.
Lebas, E., Le Friant, A., Boudon, G., Watt, S.F.L., Talling, P.J., Feuillet, N., Deplus, C., Berndt, C., Vardy, M.E., 2011. Multiple widespread landslides during the long-term evolution of a volcanic island: Insights from high-resolution seismic data, Montserrat, Lesser Antilles. Geochem. Geophys. Geosyst. 12.
Lowe, D.J., 1988. Stratigraphy, age, composition, and correlation of late Quaternary tephras interbedded with organic sediments in Waikato lakes, North Island, New Zealand. N. Z. J. Geol. Geophys. 31, 125–165.
Lowe, D.J., 2011. Tephrochronology and its application: a review. Quat. Geochronol. 6 (2), 107–153.
Lowe, D.J., Hunt, J.B., 2001. A summary of terminology used in tephra-related studies. Les Dossiers de l'Archaeo-Logis 1, 17–22.
Lowe, D.J., Shane, P.A.R., Alloway, B.V., Newnham, R.M., 2008. Fingerprints and age models for widespread New Zealand tephra marker beds erupted since 30,000 years ago: a framework for NZ-INTIMATE. Quat. Sci. Rev. 27, 95–126.
Machida, H., Arai, F., 1983. Extensive ash falls in and around the sea of Japan from large late Quaternary eruptions. J. Volcanol. Geotherm. Res. 18, 151–164.
Manga, M., Patel, A., Dufek, J., 2011. Rounding of pumice clasts during transport: field measurements and laboratory studies. Bull. Volcanol. 73 (3), 321–333.
Manville, V., Wilson, C.J.N., 2004. Vertical density currents: a review of their potential role in the deposition and interpretation of deep-sea ash layers. J. Geol. Soc. 161, 947–958.
Manville, V., Nemeth, K., Kano, K., 2009. Source to sink: a review of three decades of progress in the understanding of volcaniclastic processes, deposits, and hazards. Sediment. Geol. 220 (3–4), 136–161.
Masson, D.G., Harbitz, C.B., Wynn, R.B., Pedersen, G., Lovholt, F., 2006. Submarine landslides: processes, triggers and hazard prediction. Philos. Trans. R. Soc. A Math. Phys. Eng. Sci. 364 (1845), 2009–2039.
Matsu'ura, T., Ueno, T., Furusawa, A., 2011. Characterization and correlation of cryptotephras using major-element analyses of melt inclusions preserved in quartz in last interglacial marine sediments, southeastern Shikoku, Japan. Quat. Int. 246, 48–56.
Matthews, N.E., Smith, V.C., Costa, A., Durant, A.J., Pyle, D.M., Pearce, N.G.J., 2012. Ultra-distal tephra deposits from super-eruptions: examples from Toba, Indonesia and Taupo Volcanic Zone, New Zealand. Quat. Int. 258, 54–79.
McGuire, W.J., Howarth, R.J., Firth, C.R., Solow, A.R., Pullen, A.D., Saunders, S.J., Stewart, I.S., VitaFinzi, C., 1997. Correlation between rate of sea-level change and frequency of explosive volcanism in the Mediterranean. Nature 389 (6650), 473–476.
Melnik, O., Sparks, R.S.J., 1999. Nonlinear dynamics of lava dome extrusion. Nature 402 (6757), 37–41.
Moore, J.G., Normark, W.R., Holcomb, R.T., 1994. Giant Hawaiian landslides. Annu. Rev. Earth Planet. Sci. 22, 119–144.
Mulder, T., Alexander, J., 2001. The physical character of subaqueous sedimentary density flows and their deposits. Sedimentology 48 (2), 269–299.
Mulder, T., Cochonat, P., 1996. Classification of offshore mass movements. J. Sediment. Res. 66 (1), 43–57.
Murphy, M.D., Sparks, R.S.J., Barclay, J., Carroll, M.R., Lejeune, A.M., Brewer, T.S., Macdonald, R., Black, S., Young, S., 1998. The role of magma mixing in triggering the current eruption at the Soufrière Hills volcano, Montserrat, West Indies. Geophys. Res. Lett. 25 (18), 3433–3436.
Murphy, M.D., Sparks, R.S.J., Barclay, J., Carroll, M.R., Brewer, T.S., 2000. Remobilization of andesite magma by intrusion of mafic magma at the Soufrière Hills Volcano, Montserrat, West Indies. J. Petrol. 41 (1), 21–42.
Nederbragt, A., Dunbar, R.B., Osborn, A.T., Palmer, A., Thurow, J.W., Wagner, T., 2006. Sediment colour analysis from digital images and correlation with sediment composition. In: Rothwell, R.G. (Ed.), New Techniques in Sediment Core Analysis. Geol. Soc. Lond. Spec. Publ., pp. 99–112
Ortega-Guerrero, B., Newton, A.J., 1998. Geochemical characterisation of LatePleistocene and Holocene tephra layers from the basin of Mexico, Central Mexico. Quat. Res. 50, 90–106.
Palike, H., Shackleton, N.J., Rohl, U., 2001. Astronomical forcing in Late Eocene marine sediments. Earth Planet. Sci. Lett. 193 (3–4), 589–602.
Paterne, M., Guichard, F., Labeyrie, J., 1988. Explosive activity of the South Italian volcanoes during the past 80,000 years as determined by marine tephrochronology. J. Volcanol. Geotherm. Res. 34 (3–4), 153–172.
Piper, D.J.W., Cochonat, P., Morrison, M.L., 1999. The sequence of events around the epicentre of the 1929 Grand Banks earthquake: initiation of debris flows and turbidity current inferred from sidescan sonar. Sedimentology 46 (1), 79–97.
Pyle, D.M., Ricketts, G.D., Margari, V., van Andel, T.H., Sinitsyn, A.A., Praslov, N.D., Lisitsyn, S., 2006. Wide dispersal and deposition of distal tephra during the Pleistocene 'Campanian Ignimbrite/Y5' eruption. Italy. Quat. Sci. Rev. 25 (21–22), 2713–2728.
Rasmussen, T.L., Wastegard, S., Kuijpers, E., van Weering, T.C.E., Heinemeier, J., Thomsen, E., 2003. Stratigraphy and distribution of tephra layers in marine sediment cores from the Faeroe Islands, North Atlantic. Mar. Geol. 199 (3–4), 263–277.
Rea, J.W., 1974. The volcanic geology and petrology of Montserrat, West Indies. Geol. Soc. Lond. 130, 341–366.
Reid, R.P., Carey, S.N., Ross, D.R., 1996. Late quaternary sedimentation in the Lesser Antilles island arc. Geol. Soc. Am. Bull. 108 (1), 78–100.
Roobol, M.J., Smith, A.L., 1998. Pyroclastic stratigraphy of the Soufrière Hills volcano, Montserrat — implications for the present eruption. Geophys. Res. Lett. 25 (18), 3393–3396.
Rose, W.I., Durant, A.J., 2011. Fate of volcanic ash: aggregation and fallout. Geology 39 (9), 895–896.
Rothwell, R.G., 1992. Late quaternary evolution of the Madeira Abyssal plain, NE Atlantic. Basin Res. 4, 103–131.
Rothwell, R.G., Rack, F.R., 2006. New techniques in sediment core analysis: an introduction. In: Rothwell, R.G. (Ed.), New Techniques in Sediment Core Analysis. Geological Society of London Special Publications, pp. 1–29.
Ruddiman, W.F., Glover, L.K., 1972. Vertical mixing of ice-rafted volcanic ash in the North Atlantic sediments. Geol. Soc. Am. Bull. 83, 2817–2836.
Schindlbeck, J.C., Kutterolf, S., Freundt, A., Scudder, R.P., Pickering, K.T., Murray, R.W., 2013. Emplacement processes of submarine volcaniclastic deposits (IODP Site C0011, Nankai Trough). Mar. Geol. 343, 115–124.
Schneider, J.-L., Le Ruyet, A., Chanier, F., Buret, C., Ferrière, J., Proust, J.-N., Rosseel, J.-B., 2001. Primary or secondary distal volcaniclastic turbidites: how to make the distinction? An example from the Miocene of New Zealand (Mahia Peninsula, North Island). Sediment. Geol. 145, 1–22.
Sigurdsson, H., Sparks, R.S.J., Carey, S.N., Huang, T.C., 1980. Volcanogenic sedimentation in the Lesser Antilles arc. J. Geol. 88 (5), 523–540.
Smith, A.L., Roobol, M.J., Schellekens, J.H., Mattioli, G.S., 2007. Prehistoric stratigraphy of the Soufrière Hills–South Soufrière Hills volcanic complex, Montserrat, West Indies. J. Geol. 115, 115–127.
Smith, V.C., Pearce, N.J.G., Matthews, N.E., Westgate, J.A., Petraglia, M.D., Haslam, M., Lane, C.S., Korisettar, R., Pal, J.N., 2011. Geochemical fingerprinting of the widespread Toba tephra using biotite compositions. Quat. Int. 246, 97–104.
Sparks, R.S.J., Burski, M.I., Carey, S.N., Gilbert, J.S., Glaze, L.S., Sigurdsson, H., Woods, A.W. (Eds.), 1997. Volcanic Plumes. Wiley, Chichester (1–590 pp.).
Sparks, R.S.J., Young, S.R., Barclay, J., Calder, E.S., Cole, P., Darroux, B., Davies, M.A., Druitt, T. H., Harford, C., Herd, R., James, M., Lejeune, A.M., Loughlin, S., Norton, G., Skerrit, G., Stasiuk, M.V., Stevens, N.S., Toothill, J., Wadge, G., Watts, R., 1998. Magma production and growth of the lava dome of the Soufrière Hills Volcano, Montserrat, West Indies: November 1995 to December 1997. Geophys. Res. Lett. 25 (18), 3421–3424.
Sparks, R.S.J., Murphy, M.D., Lejeune, A.M., Watts, R.B., Barclay, J., Young, S.R., 2000. Control on the emplacement of the Andesite Lava Dome of the Soufriere Hills volcano, Montserrat by degassing-induced crystallization. Terra Nova 12 (1), 14–20.
Stanton, T., Snowball, I., Zillen, L., Wastegard, S., 2010. Validating a Swedish varve chronology using radiocarbon, palaeomagnetic secular variation, lead pollution history and statistical correlation. Quat. Geochronol. 5 (6), 611–624.
Stevenson, J.A., Loughlin, S., Rae, C., Thordarson, T., Milodowski, A.E., Gilbert, J.S., Harangi, S., Lukács, R., Højgaard, B., Árting, U., Pyne-O'Donnell, S., MacLeod, A., Whitney, B., Cassidy, M, 2012. Distal deposition of tephra from the Eyjafjallajokull 2010 summit eruption. J. Geophys. Res. Solid Earth 117.
Straub, S.M., Schmincke, H.U., 1998. Evaluating the tephra input into Pacific Ocean sediments: distribution in space and time. Geol. Rundsch. 87 (3), 461–476.
Takemura, K., Hayashida, A., Okamura, M., Matsuoka, H., Ali, M., Kuniko, Y., Torii, M., 2000. Stratigraphy of multiple piston-core sediments for the last 30,000 years from Lake Biwa, Japan. J. Paleolimnol. 23 (2), 185–199.
Talling, P.J., Wynn, R.B., Masson, D.G., Frenz, M., Cronin, B.T., Schiebel, R., Akhmetzhanov, A.M., Dallmeier-Tiessen, S., Benetti, S., Weaver, P.P.E., Georgiopoulou, A., Zuehlsdorff, C., Amy, L.A., 2007. Onset of submarine debris flow deposition far from original giant landslide. Nature 450 (7169), 541–544.
Trofimovs, J., Amy, L., Boudon, G., Deplus, C., Doyle, E., Fournier, N., Hart, M.B., Komorowski, J.C., Le Friant, A., Lock, E.J., Pudsey, C., Ryan, G., Sparks, R.S.J., Talling, P. J., 2006. Submarine pyroclastic deposits formed at the Soufrière Hills volcano, Montserrat (1995–2003): what happens when pyroclastic flows enter the ocean? Geology 34 (7), 549–552.
Trofimovs, J., Sparks, R.S.J., Talling, P.J., 2008. Anatomy of a submarine pyroclastic flow and associated turbidity current: July 2003 dome collapse, Soufrière Hills volcano, Montserrat, West Indies. Sedimentology 55 (3), 617–634.

Trofimovs, J., Fisher, J.K., MacDonald, H.A., Talling, P.J., Sparks, R.S.J., Hart, M.B., Smart, C.W., Boudon, G., Deplus, C., Komorowski, J.C., Le Friant, A., Moreton, S.G., Leng, M.J., 2010. Evidence for carbonate platform failure during rapid sea-level rise; ca 14 000 year old bioclastic flow deposits in the Lesser Antilles. Sedimentology 57 (3), 735–759.

Trofimovs, J., Talling, P.J., Fisher, J.K., Sparks, R.S.J., Watt, S.F.L., Cassidy, M., Hart, M.B., Smart, C., Le Friant, W.A., Moreton, S.G., Leng, M.J., 2013. Timing, origin and emplacement dynamics of mass flows offshore of SE Montserrat in the last 110 ka: implications for landslide and tsunami hazards, eruption history, and volcanic island evolution. Geochem. Geophys. Geosyst. 14 (2), 385–406.

Turner, M.B., Cronin, S.J., Stewart, R.B., Bebbington, M., Smith, I.E.M., 2008. Using titanomagnetite textures to elucidate volcanic eruption histories. Geology 36 (1), 31–34.

Turney, C.S.M., Lowe, J.J., Davies, S.M., Hall, V., Lowe, D.J., Wastegard, S., Hoek, W.Z., Alloway, B., 2004. Tephrochronology of last termination sequences in Europe: a protocol for improved analytical precision and robust correlation procedures (a joint SCOTAV-INTIMATE proposal). J. Quat. Sci. 19, 111–120.

Van Daele, M., Moernaut, J., Silversmit, G., Schmidt, S., Fontijn, K., Heirman, K., Vandoorne, W., De Clercq, M., Van Acker, J., Wolff, C., et al., 2014. The 600 yr eruptive history of Villarrica Volcano (Chile) revealed by annually laminated lake sediments. Geol. Soc. Am. Bull. http://dx.doi.org/10.1130/B30798.1.

Vogel, H., Zanchetta, G., Sulpizio, R., Wagner, B., Nowaczyk, N., 2010. A tephrostratigraphic record for the last glacial–interglacial cycle from Lake Ohrid, Albania and Macedonia. J. Quat. Sci. 25 (3), 320–338.

Voight, B., Sparks, R.S.J., Miller, A.D., Stewart, R.C., Hoblitt, R.P., Clarke, A., Ewart, J., Aspinall, W.P., Baptie, B., Calder, E.S., Cole, P., Druitt, T.H., Hartford, C., Herd, R.A., Jackson, P., Lejeune, A.M., Lockhart, A.B., Loughlin, S.C., Luckett, R., Lynch, L., Norton, G.E., Robertson, R., Watson, I.M., Watts, R., Young, S.R., 1999. Magma flow instability and cyclic activity at Soufrière Hills Volcano, Montserrat, British West Indies. Science 283 (5405), 1138–1142.

Wadge, G., 1984. Comparison of volcanic production-rates and subduction rates in the Lesser Anitlles and Central America. Geology 12 (9), 555–558.

Walker, R.G., 1969. Geometric analysis of ripple-drift cross-lamination. Can. J. Earth Sci. 6, 683–691.

Walker, G.P.L., Wilson, L., Bowell, E.L.G., 1971. Explosive volcanic eruptions—I. The rate of fall of pyroclasts. Geophys. J. Roy. Astron. Soc. 22 (4), 377.

Wastegard, S., Davies, S.M., 2009. An overview of distal tephrochronology in northern Europe during the last 1000 years. J. Quat. Sci. 24 (5), 500–512.

Watt, S.F.L., Pyle, D.M., Mather, T.A., Martin, R.S., Matthews, N.E., 2009. Fallout and distribution of volcanic ash over Argentina following the May 2008 explosive eruption of Chaitén, Chile. J. Geophys. Res. 114, B04207.

Watt, S.F.L., Talling, P.J., Vardy, M.E., Heller, V., Huhnerbach, V., Urlaub, Morelia, Sarkar, Sudipta, Masson, D.G., Henstock, T.J., Minshull, T.A., Paulatto, M., Le Friant, A., Lebas, E., Berndt, C., Crutchley, G., Karstens, J., Stinton, A., Maeno, F., 2012a. Combinations of volcanic-flank and seafloor-sediment failure offshore Montserrat, and their implications for tsunami generation. Earth Planet. Sci. Lett. 319–320, 228–240.

Watt, S.F.L., Talling, P.J., Vardy, M.E., Masson, D.M., Henstock, T.J., Hühnerbach, V., Minsull, T.A., Urlaub, M., Lebas, E., Le Friant, A., Berndt, C., Crutchley, G.J., Karstens, J., 2012b. Widespread and progressive seafloor-sediment failure following volcanic debris avalanche emplacement: landslide dynamics and timing offshore Montserrat, Lesser Antilles. Mar. Geol. 323–325, 69–94.

Watt, S.F.L., Pyle, D.M., Mather, T.A., 2013. The volcanic response to deglaciation: evidence from glaciated arcs and a reassessment of global eruption records. Earth Sci. Rev. 122, 77–102.

Weltje, G.J., Tjallingii, R., 2008. Calibration of XRF core scanners for quantitative geochemical logging of sediment cores: theory and application. Earth Planet. Sci. Lett. 274 (3–4), 423–438.

Wetzel, A., 2009. The preservation potential of ash layers in the deep-sea: the example of the 1991-Pinatubo ash in the South China Sea. Sedimentology 56 (7), 1992–2009.

Wiesner, M.G., Wetzel, A., Catane, S.G., Listanco, E.L., Mirabueno, H.T., 2004. Grain size, areal thickness distribution and controls on sedimentation of the 1991 Mount Pinatubo tephra layer in the South China Sea. Bull. Volcanol. 66 (3), 226–242.

Wilson, L., Walker, G.P.L., 1987. Explosive volcanic-eruptions 6. Ejecta dispersal in plinian eruptions — the control of eruption conditions and atmospheric properties. Geophys. J. R. Astron. Soc. 89 (2), 657–679.

Wulf, S., Kraml, M., Brauer, A., Keller, J., Negendank, J.F.W., 2004. Tephrochronology of the 100 ka lacustrine sediment record of Lago Grandedi Monticchio (southern Italy). Quat. Int. 122, 7–30.

Wulf, S., Keller, J., Paterne, M., Mingram, J., Lauterbach, S., Opitz, S., Sottili, G., Giaccio, B., Albert, P.G., Satow, C., Tomlinson, E.L., Viccaro, M., Brauer, A., 2012. The 100–133 ka record of Italian explosive volcanism and revised tephrochronology of Lago Grande di Monticchio. Quat. Sci. Rev. 58, 104–123.

Wynn, R.B., Masson, D.G., 2003. Canary island landslides and tsunami generation: can we use turbidite deposits to interpret landslide processes. In: Mienert, J.L.J. (Ed.), Submarine Mass Movements and Their Consequences. Kluwer Academic Publishers, Dordrecht, Netherlands, pp. 325–332.

Young, S.R., Sparks, R.S.J., Aspinall, W.P., Lynch, L.L., Miller, A.D., Robertson, R.E.A., Shepherd, J.B., 1998. Overview of the eruption of Soufrière Hills volcano, Montserrat, 18 July 1995 to December 1997. Geophys. Res. Lett. 25 (18), 3389–3392.

Zellmer, G.F., Hawkesworth, C.J., Sparks, R.S.J., Thomas, L.E., Harford, C.L., Brewer, T.S., Loughlin, S.C., 2003. Geochemical evolution of the Soufrière Hills volcano, Montserrat, Lesser Antilles volcanic arc. J. Petrol. 44 (8), 1349–1374.

Zielinski, G.A., Dibb, J.E., Yang, Q.Z., Mayewski, P.A., Whitlow, S., Twickler, M.S., Germani, M.S., 1997. Assessment of the record of the 1982 El Chichon eruption as preserved in Greenland snow. J. Geophys. Res.-Atmos. 102 (D25), 30031–30045.